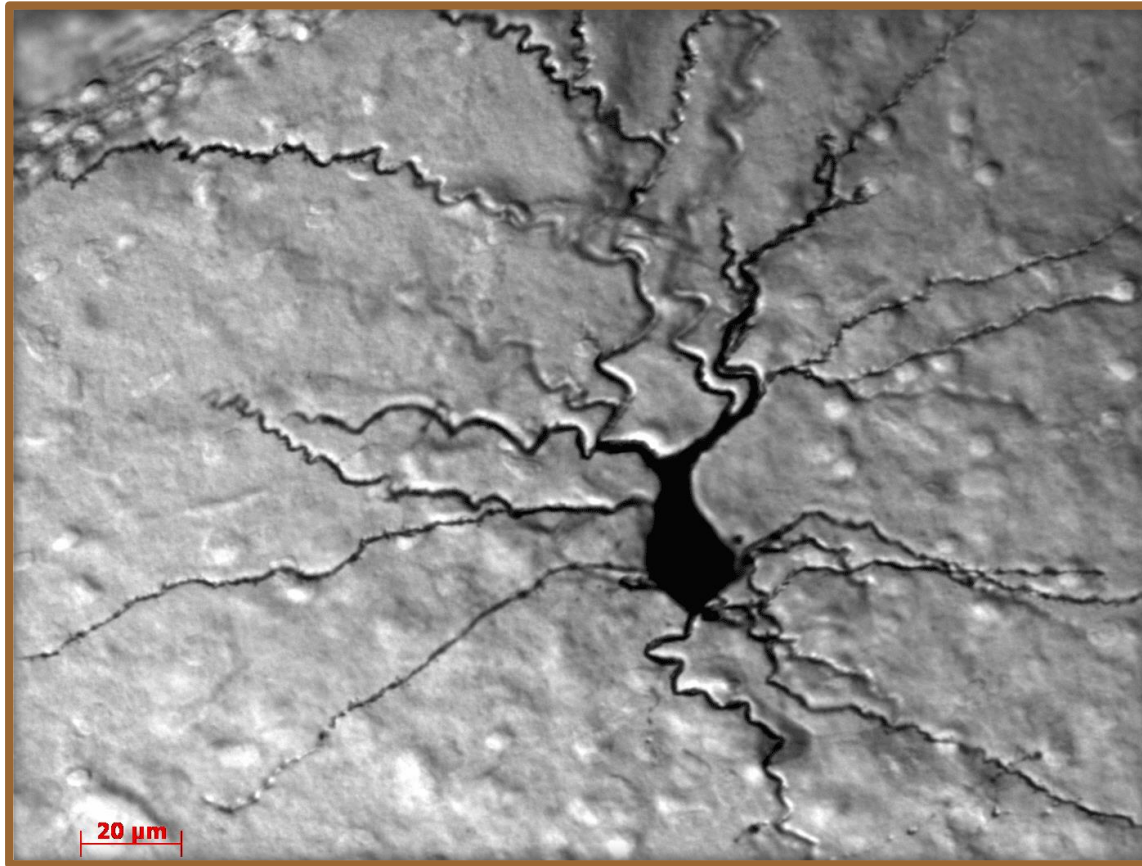


# The neuron



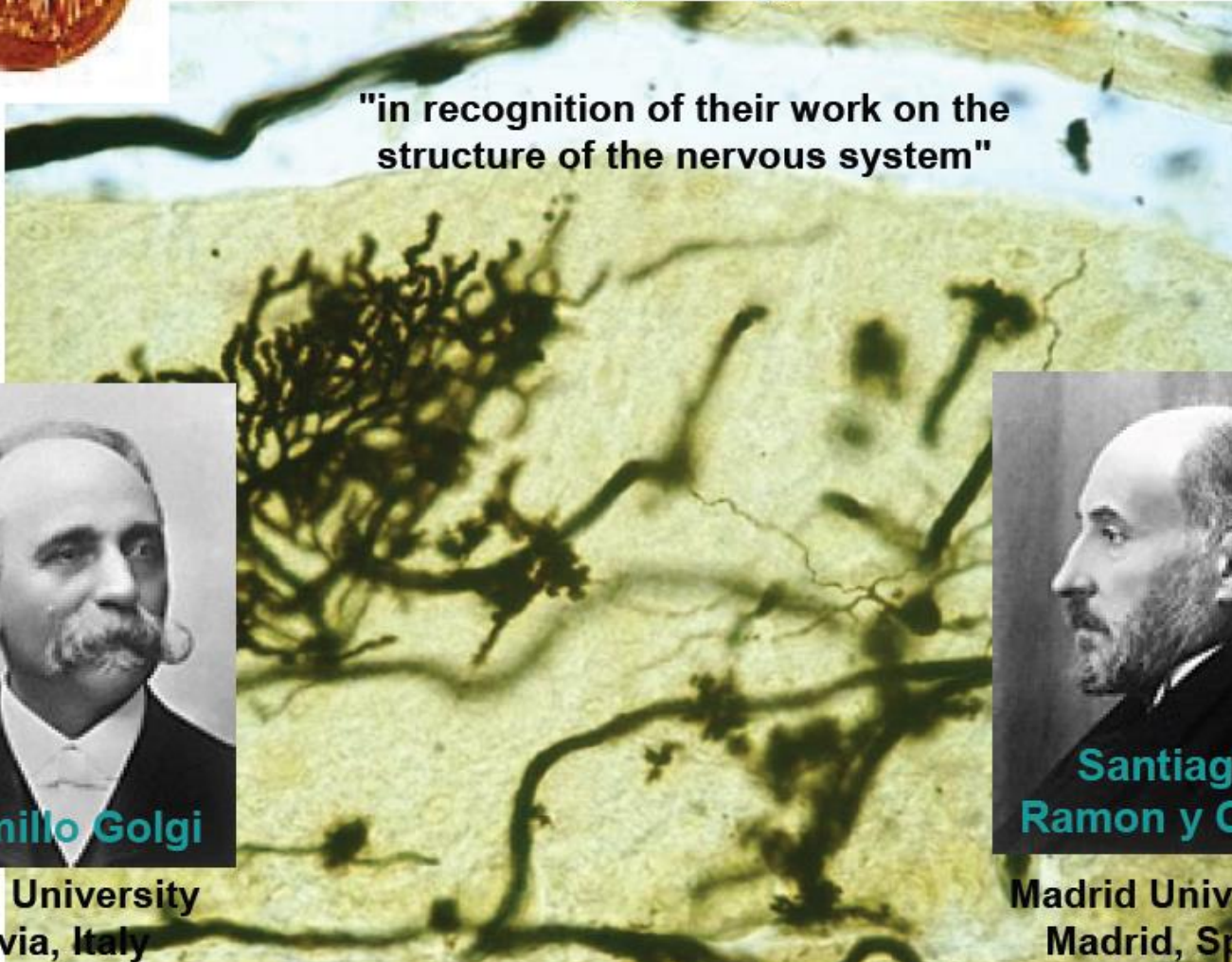
Biocytin labeled pyramidal neuron recorded in piriform cortex

# Discovery of the neuron



The Nobel Prize in Physiology or Medicine 1906

"in recognition of their work on the structure of the nervous system"



**Camillo Golgi**

Pavia University  
Pavia, Italy



**Santiago  
Ramon y Cajal**

Madrid University  
Madrid, Spain

## The nervous system as a diffuse reticular syncytium?

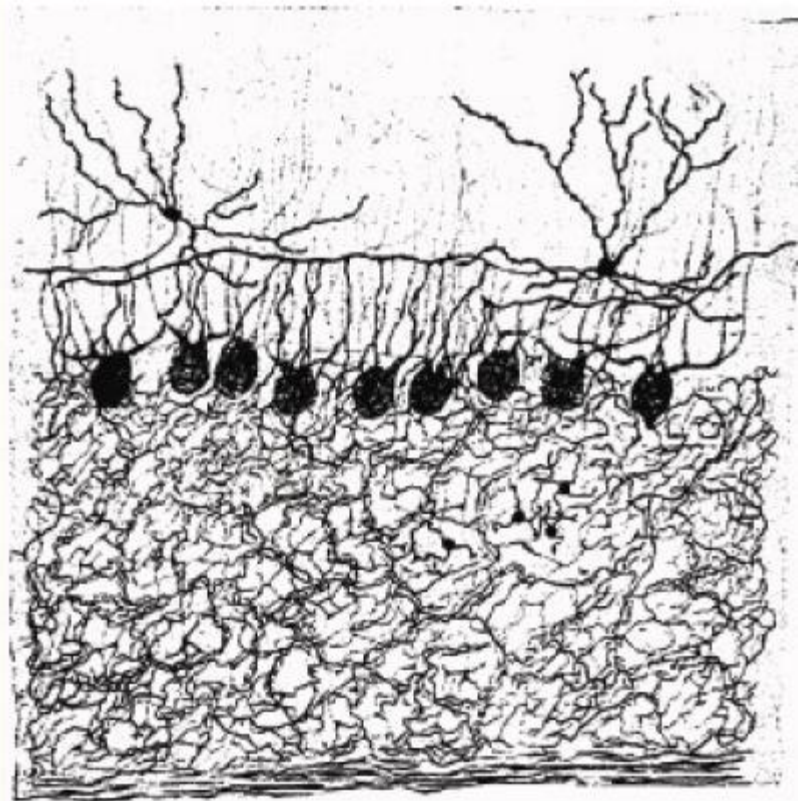
(i.e. a mass of cytoplasm with many nuclei but no internal cell boundaries)

Camillo Golgi

Nobel Lecture December 11, 1906

The Neuron Doctrine- theory and facts.

“..Far from being able to accept the idea of the individuality and independence of each nerve element, I have never had reason, up to now, to give up the concept which I have always stressed, that nerve cells, instead of working individually, act together, so that we must think that several groups of elements exercise a cumulative effect on the peripheral organs through whole bundles of fibers.”

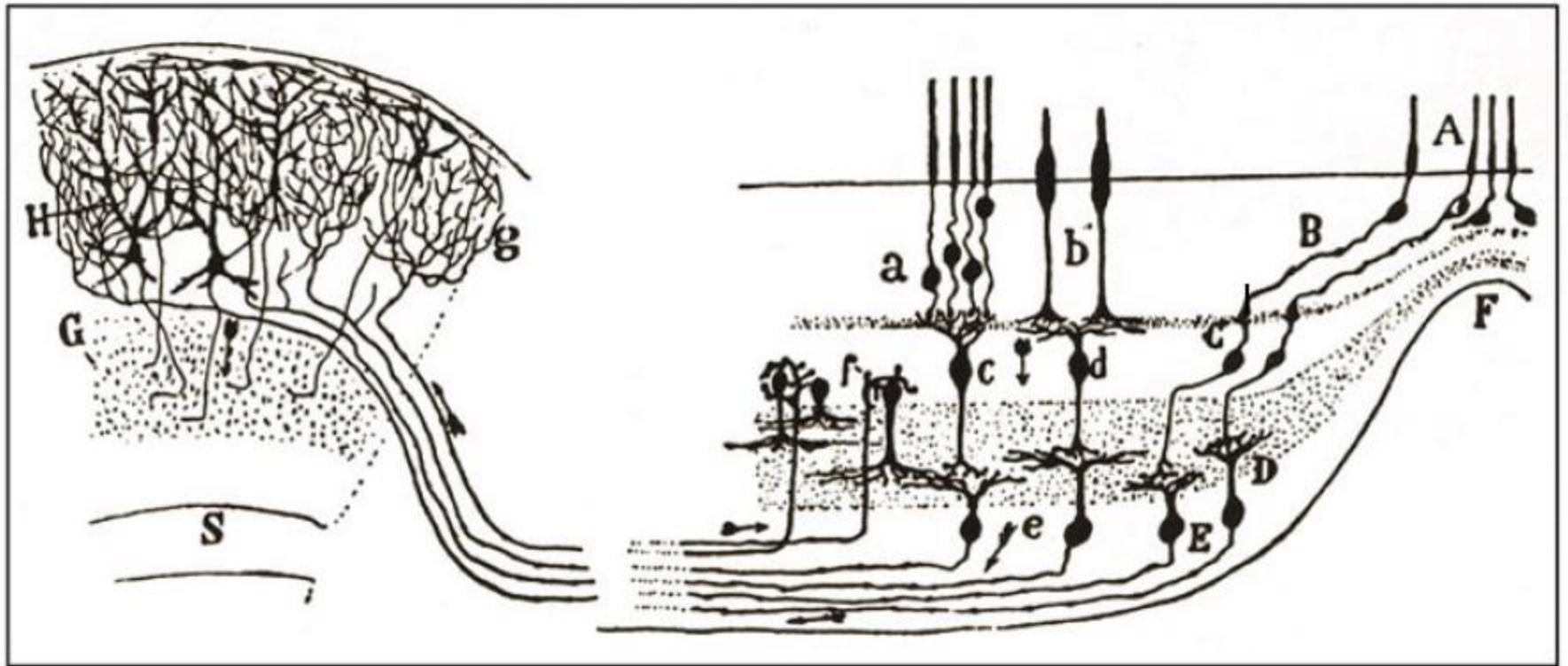


## The Neuron Doctrine: (Santiago Ramon y Cajal)

Neurons are cells.

Each is an individual entity anatomically, embryologically, and functionally.

Also: Neurons have a functional polarity.

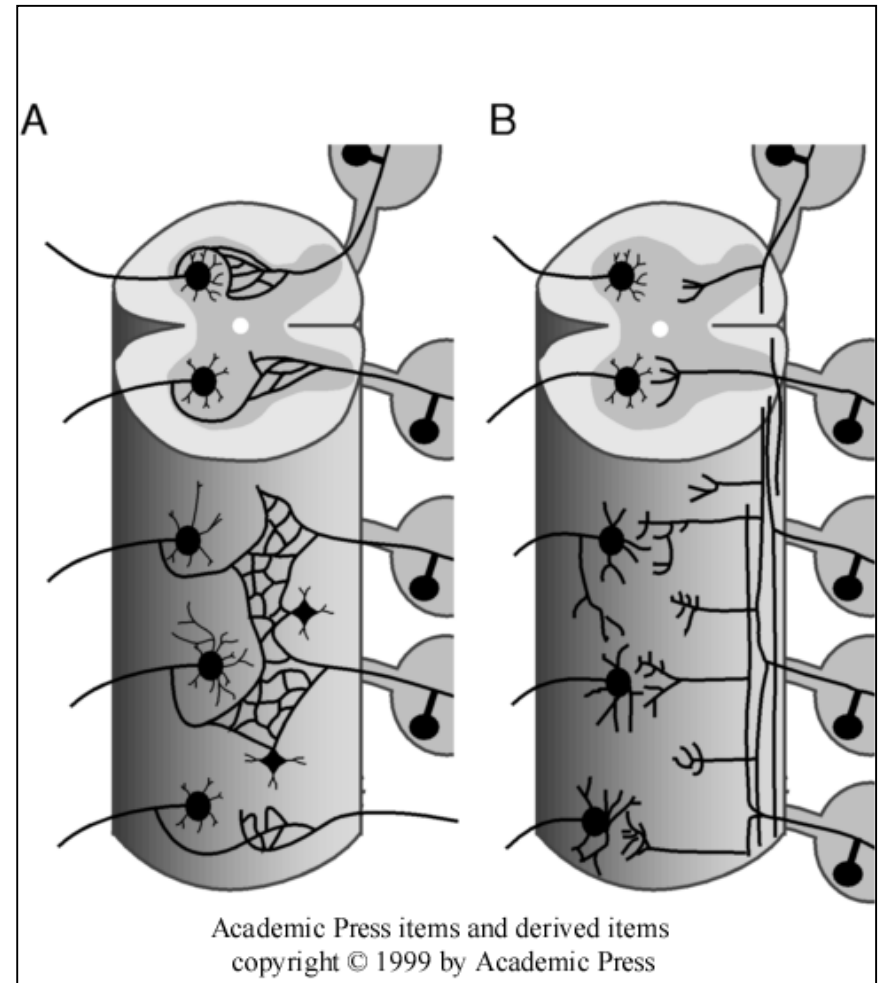


(A) Reticularist Doctrine

(B) Neuron Doctrine

Exception.....

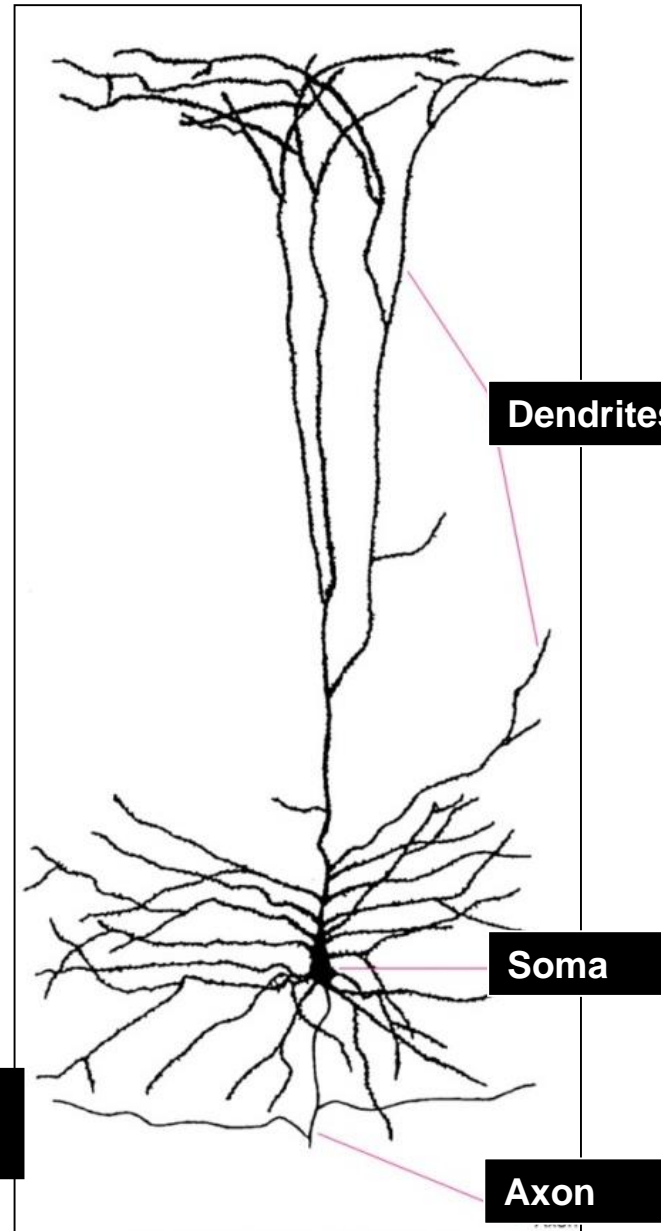
....GAP JUNCTIONS  
between neurons



**FIGURE 2** The nervous system is a reticulum versus the neuron doctrine. (A) Proponents of the reticularist's view of the nervous system believed that neurons are physically connected to one another, forming an uninterrupted network. (B) The neuron doctrine, in contrast, considers each neuron an individual entity that communicates with target cells across an appropriate intercellular gap. Adapted from Cajal (1911–1913).

# Neuronal shape

Pyramidal neuron  
(multipolar)



Dendrites

Soma

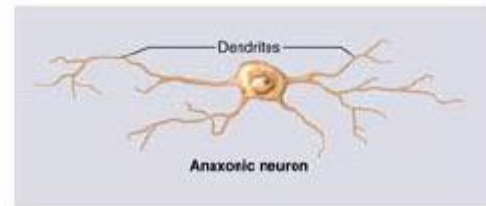
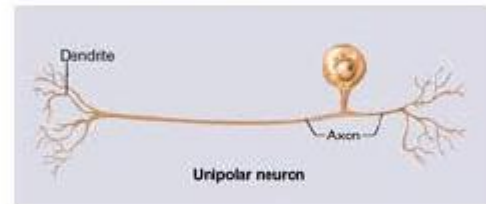
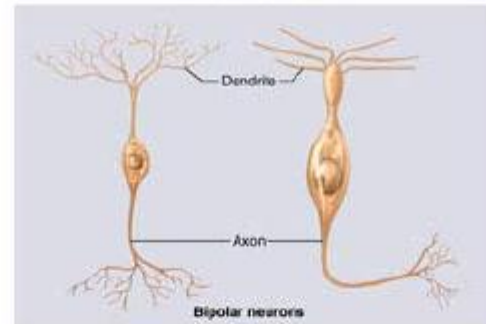
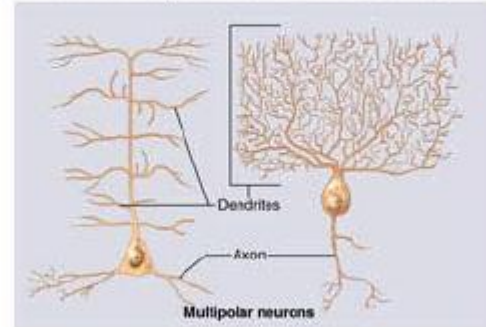
Axon

# Variation in Neural Structure

Copyright © The McGraw-Hill Companies, Inc. Permission required for reproduction or display.

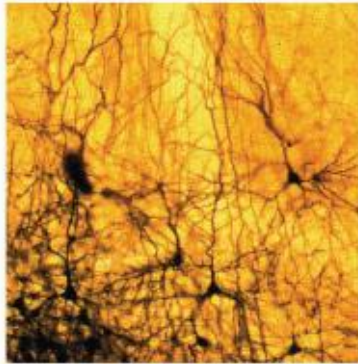
## Basic classification of neurons

- **Multipolar neuron**
  - most common
  - many dendrites/one axon
- **Bipolar neuron**
  - one dendrite/one axon
  - olfactory, retina, ear
- **Unipolar neuron (pseudounipolar)**
  - sensory from skin and organs to spinal cord
- **Anaxonic neuron**
  - many dendrites/no axon
  - help in visual processes

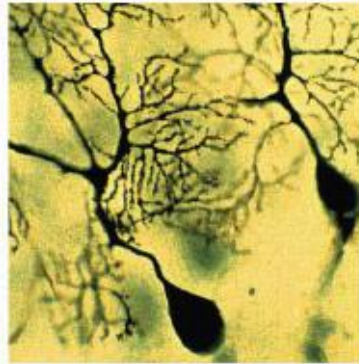


# Studying structure

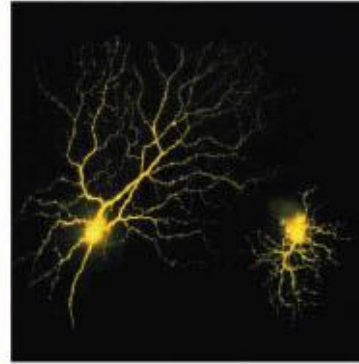
(A) Golgi stain/  
cortical neurons



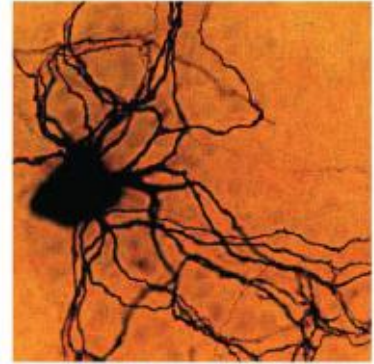
(B) Golgi stain/  
Purkinje neurons



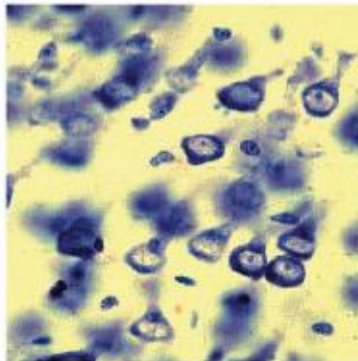
(C) Dye injection/  
retinal neurons



(D) HRP (enzyme) injection/  
autonomic neuron

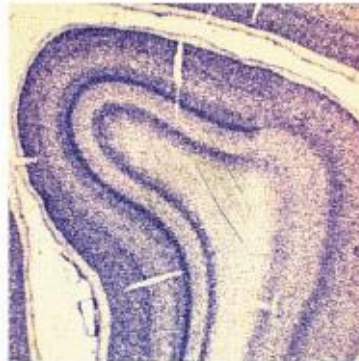


(E)



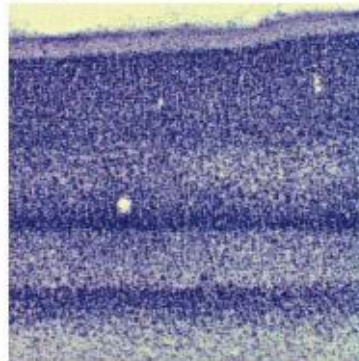
Cresyl violet/RNA/  
cortical neurons

(F)



Nissl stain/RNA/  
cortical neurons

(G)



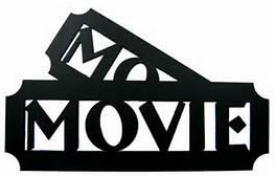
(H)



Nissl stain/  
olfactory bulb

**NEUROSCIENCE, Fourth Edition, Figure 1.6**

© 2008 Sinauer Associates, Inc.



<https://www.jove.com/science-education/5204/an-introduction-to-neuroanatomy>

<https://www.jove.com/science-education/5206/histological-staining-of-neural-tissue>



1. Who was the first person to publish a description of brain anatomy?

- A) Wilder Penfield
- B) Korbinian Brodman
- C) Thomas Willis
- D) Andreas Vesalius

2. Who developed a staining technique to visualize single neurons and in what year?

- A) Korbinian Brodman in 1909
- B) Camillo Golgi in 1873
- C) Andres Vesalius in 1906
- D) Santiago Ramón y Cajal in 1888

4. Which of the following terms most appropriately refers to the microscopic arrangement of neurons?

- A) Neurogenetics
- B) Cytoarchitecture
- C) Neuroplasticity
- D) Neurodegeneration

3.

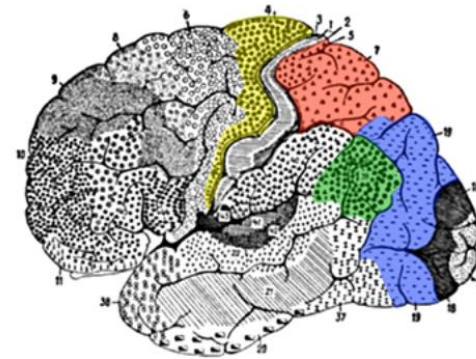


Figure 1 - Map of the Human Brain

In Figure 1, how were the various highlighted regions of the brain first distinguished from each other?

- A) By their unique cellular architecture.
- B) By their different motor functions.
- C) By their different sensory functions.
- D) By their sensitivity to neural stains.

5.

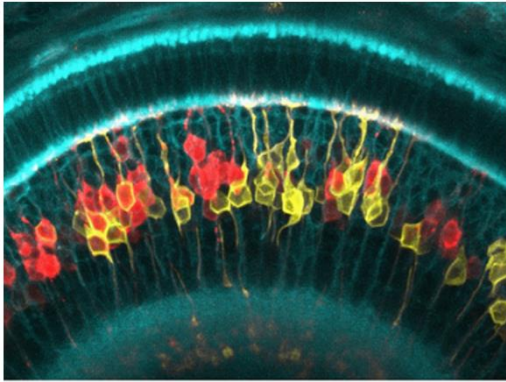


Figure 3 - Different Neurons Stained by Different Tracers

Which methodology made it possible to capture the image in Figure 3?

- A) The Golgi stain
- B) Dye injection
- C) Fluorescence microscopy
- D) Magnetic resonance imaging

6.

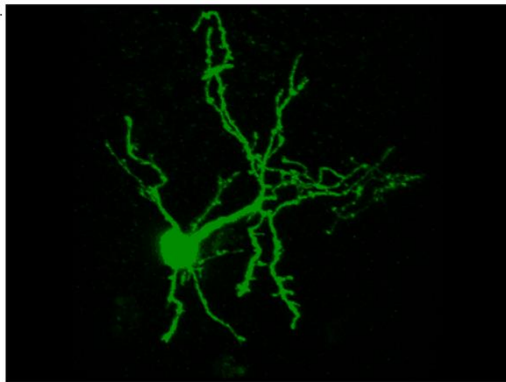


Figure 4 - 3D Reconstruction of Fluorescently Labeled Neuron

\_\_\_\_\_ microscopy allows for the creation of images seen in Figure 4.

- A) Confocal
- B) 2-Photon
- C) Fluorescence
- D) Electron

7.

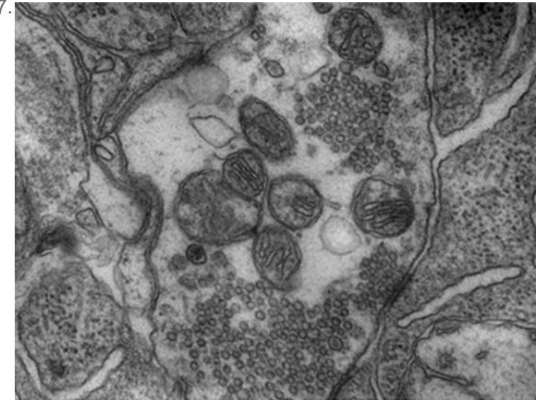


Figure 5 - Organelles in a Synaptic Terminal

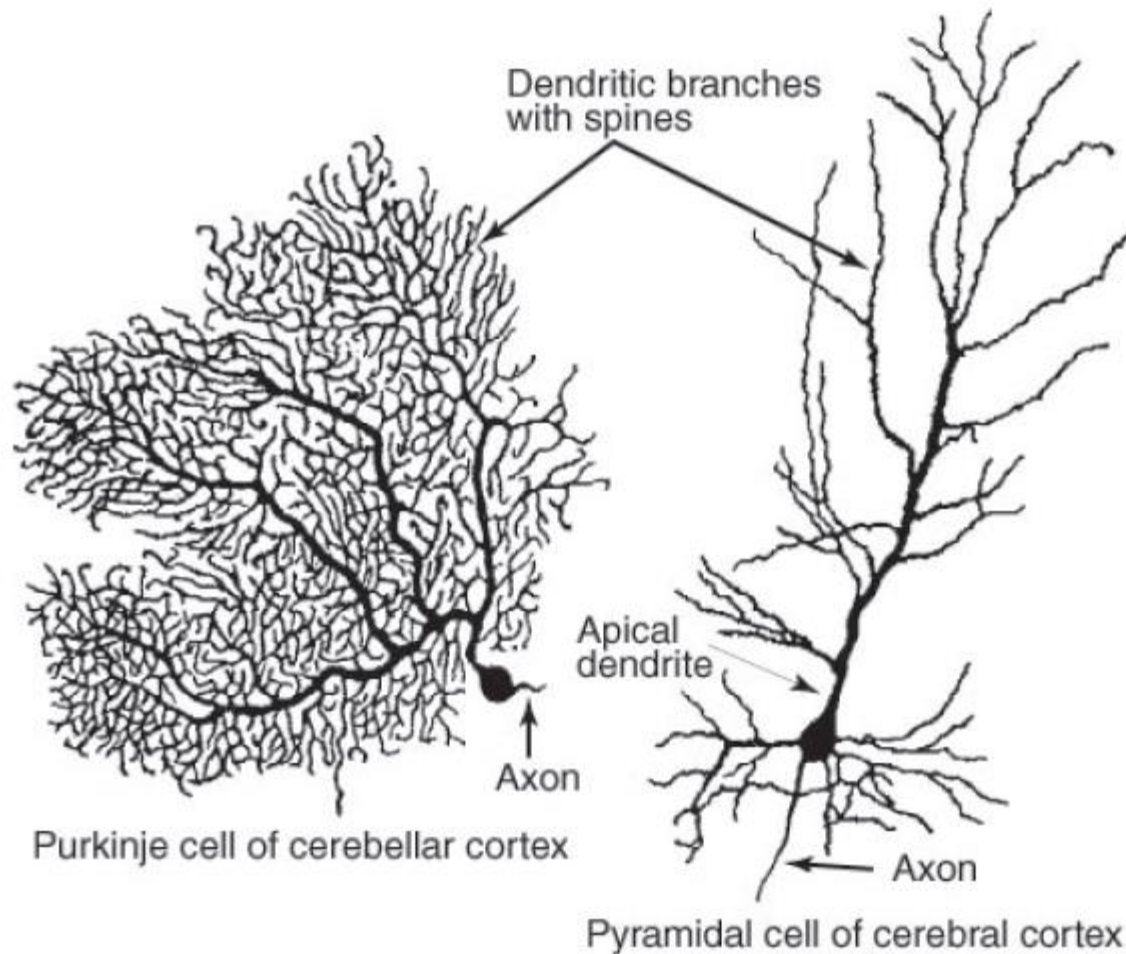
The image in Figure 5 was generated using \_\_\_\_\_ microscopy.

- A) confocal
- B) electron
- C) 2-photon
- D) atomic force

8. Which of the following techniques is NOT a potential application of stereotaxic surgery?

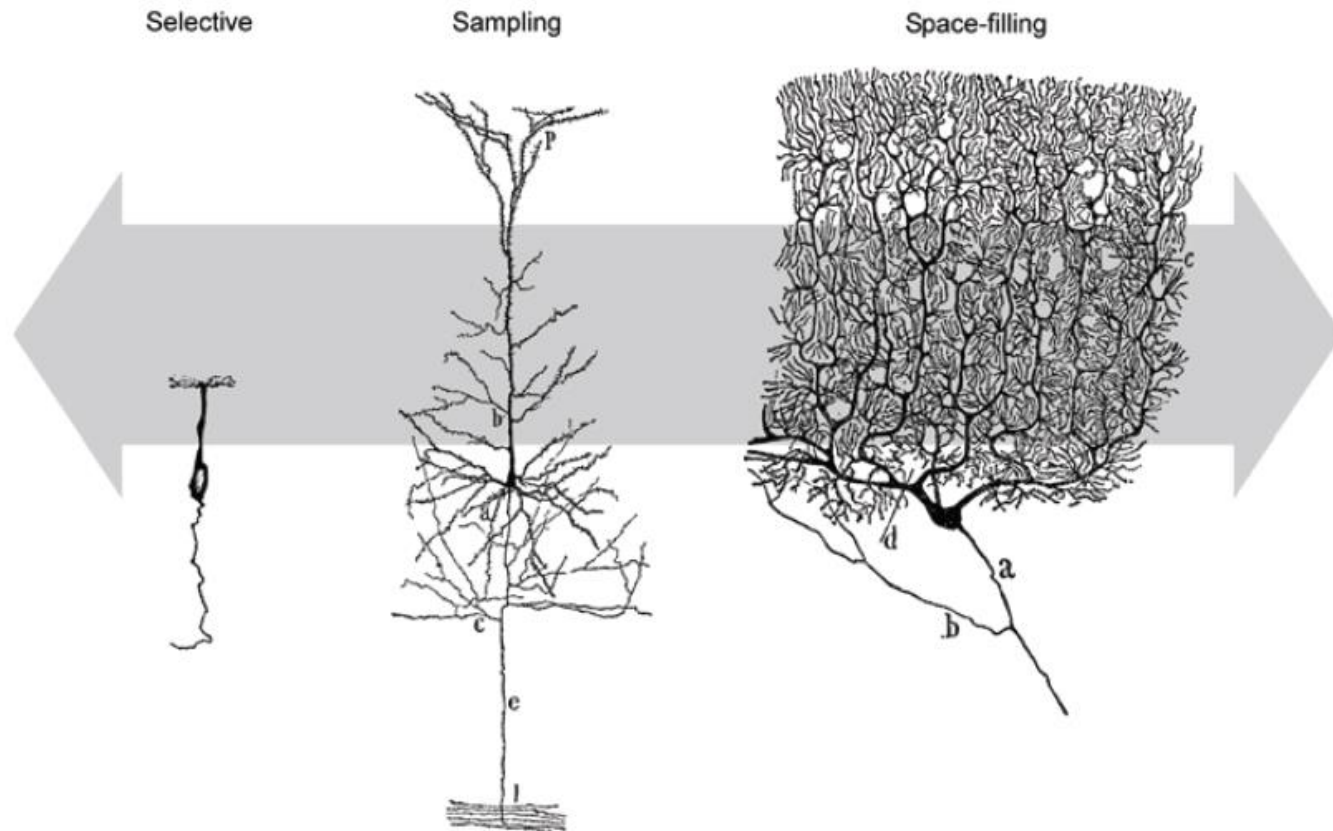
- A) Injection of drugs
- B) Generation of lesions
- C) Neuronal cell culture
- D) Delivery of electrical stimulation

# Morphology of vertebrate multipolar neurons is highly variable





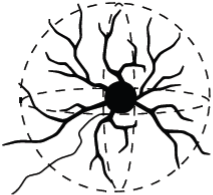
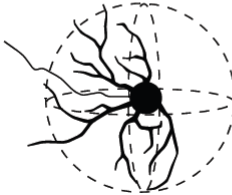

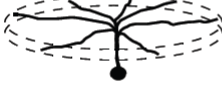

# Differences in arbor density reflect differences in connectivity

Fiala & Harris, 1999  
Dendrite structure; in  
"Dendrites", Oxford Univ  
Press


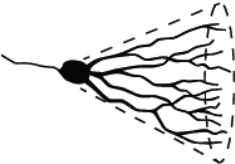
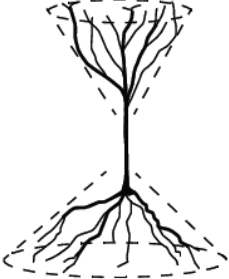



**Fig. 1.5** The densities of dendritic arbors lie on a continuum of values. Differences in arbor density reflect differences in connectivity. At one extreme are selective arborizations in which each dendrite connects the cell body to a single remote target. An olfactory sensory cell is used to illustrate this. At the other extreme lie space-filling arborizations in which the dendrites cover a region, as with the cerebellar Purkinje cell. Intermediate arbor densities are referred to as sampling arborizations, as demonstrated by a pyramidal cell from cerebral cortex. (Drawings of neurons from Ramón y Cajal, 1995.)

# Characteristic arborization patterns

Pattern	Characteristics	Examples
<b>Adendritic</b> 	Cell body lacks dendrites	Dorsal root ganglion cells Sympathetic ganglion cells
<b>Spindle radiation</b> 	Two dendrites emerge from opposite poles of the cell body and have few branches	Lugaro cells Bipolar cells of cortex
<b>Spherical radiation</b> <b>Stellate</b> 	Dendrites radiate in all directions from cell body	Spinal neurons Neurons of subcortical nuclei (e.g. inferior olive, pons, thalamus, striatum) Cerebellar granule cells
<b>Partial</b> 	Dendrites radiate from cell body in directions restricted to a part of a sphere	Neurons at edges of "closed" nuclei (e.g. Clarke's column, inferior olive, vestibular nuclei)
<b>Laminar radiation</b> <b>Planar</b> 	Dendrites radiate from cell body in all directions within a thin domain	Retinal horizontal cells
<b>Offset</b> 	Plane of radial dendrites offset from cell body by one or more stems	Retinal ganglion cells
<b>Multi</b> 	Cell has multiple layers of radial dendrites	Retinal amacrine cells

# Characteristic arborization patterns

Pattern	Characteristics	Examples
<b>Cylindrical radiation</b> 	Dendrites ramify from a central soma or dendrite in a thick cylindrical (disk-shaped) domain	Pallidal neurons Reticular neurons
<b>Conical radiation</b> 	Dendrites radiate from cell body or apical stem within a cone or paraboloid	Granule cells of dentate gyrus and olfactory bulb Primary dendrites of mitral cells of olfactory bulb Semilunar cells of piriform cortex
<b>Biconical radiation</b> 	Dendrites radiate in opposite directions from the cell body	Bitufted, double bouquet, and pyramidal cells of cerebral cortex Vertical cells of superior colliculus
<b>Fan radiation</b> 	One or a few dendrites radiate from cell body in a flat fan shape	Cerebellar Purkinje cells

# What changes among the dendrites ?

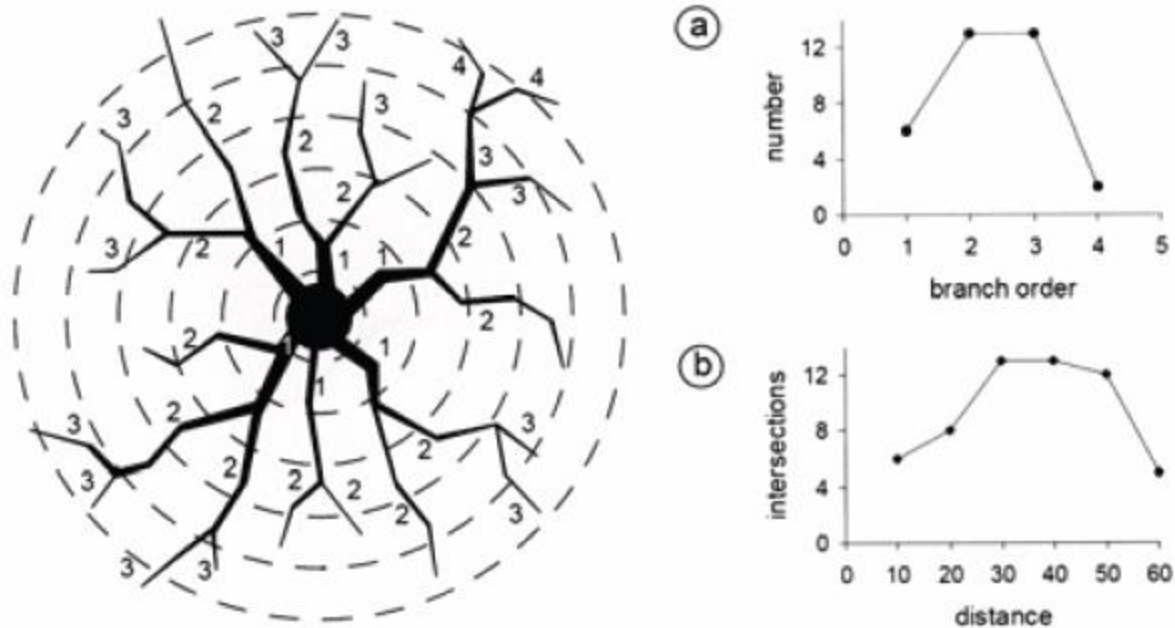
Table 1.1 Typical dimensions of dendrites for a few types of neurons

Neuron	Average soma diameter (μm)	Number of dendrites at soma	Proximal dendrite diameter (μm)	Number of branch points	Distal dendrite diameter (μm)	Dendrite extent* (μm)	Total dendritic length (μm)
Cerebellar granule cell (cat)	7	4	1	0	0.2-2	15	60
Starburst amacrine cell (rhesus)	9	1	1	40	0.2-2	120	—
Dentate gyrus granule cell (rat)	14	2	3	14	0.5-1	300	3200
CA1 pyramidal cell (rat)	21						11 900
basal dendrites		5	1	30	0.5-1	130	5500
stratum radiatum		1	3	30	0.25-1	110	4100
stratum lacunosum-moleculare				15	0.25-1	500	2300
Cerebellar Purkinje cell (guinea pig)	25	1	3	440	0.8-2.2	200	9100
Principal cell of globus pallidus (human)	33	4	4	12	0.3-0.5	1000	7600
Meynert cell of visual cortex (macaque)	35						15 400
basal dendrites		5	3	—	—	250	10 200
apical dendrites		1	4	15	2-3	1800	5200
Spinal a-motoneuron (cat)	58	11	8	120	0.5-1.5	1100	52 000

\* The average distance from the cell body to the tips of the longest dendrites.

Sources: Ito (1984); Mariani (1990); Claiborne et al. (1990); Bannister and Larkman (1995a); Rapp et al. (1994); Palay (1978); Yelnik et al. (1984); Ulfhake and Kellerth (1981)

# Methods for measuring dendritic complexity



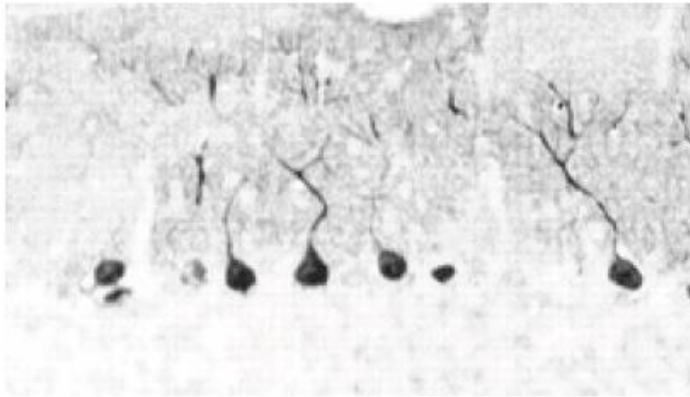
**Fig. 1.4** Methods for characterizing dendritic branching. (a) A plot of the number of branches of each order using the centrifugal method of branch ordering. The *Strahler method* is similar but the dendritic tips are order 1 and branch numbers increase sequentially toward the soma. (b) A *Sholl plot* showing the number of intersections of the dendritic tree with circles of increasing radius from the center of the dendritic arbor. When three-dimensional data are available, concentric spheres are used rather than these circles centered on a two-dimensional projection of the neuron.



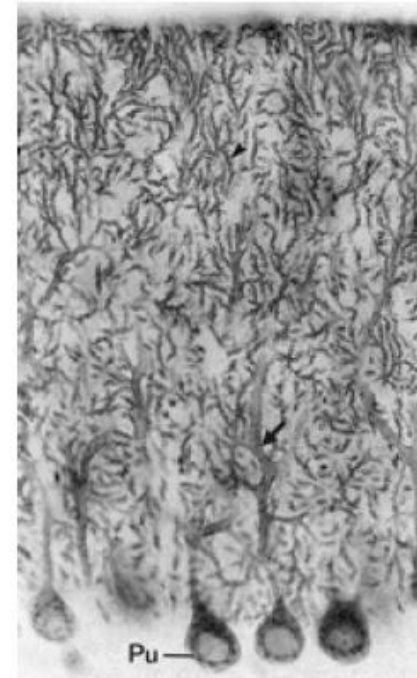
# Functional classification of neurons

- **Sensory (afferent) neurons**
  - detect changes in body and external environment
  - information transmitted into brain or spinal cord
- **Interneurons (association neurons)** • **Projection neurons**  
• **Local circuit neurons**
  - lie between sensory and motor pathways in CNS
  - 90% of our neurons are interneurons
  - process, store and retrieve information
- **Motor (efferent) neuron**
  - send signals out to muscles and gland cells
  - organs that carry out responses called effectors

# Neurons can also be identified by immunocytochemistry

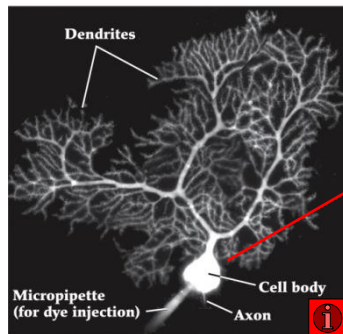
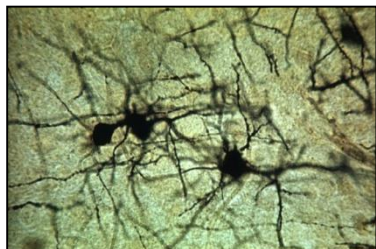
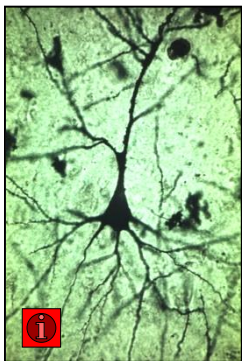
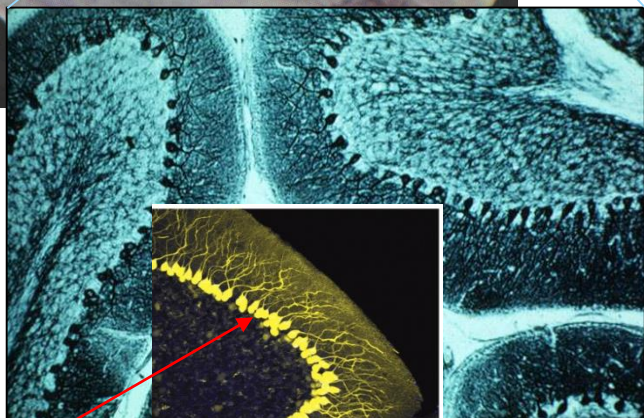
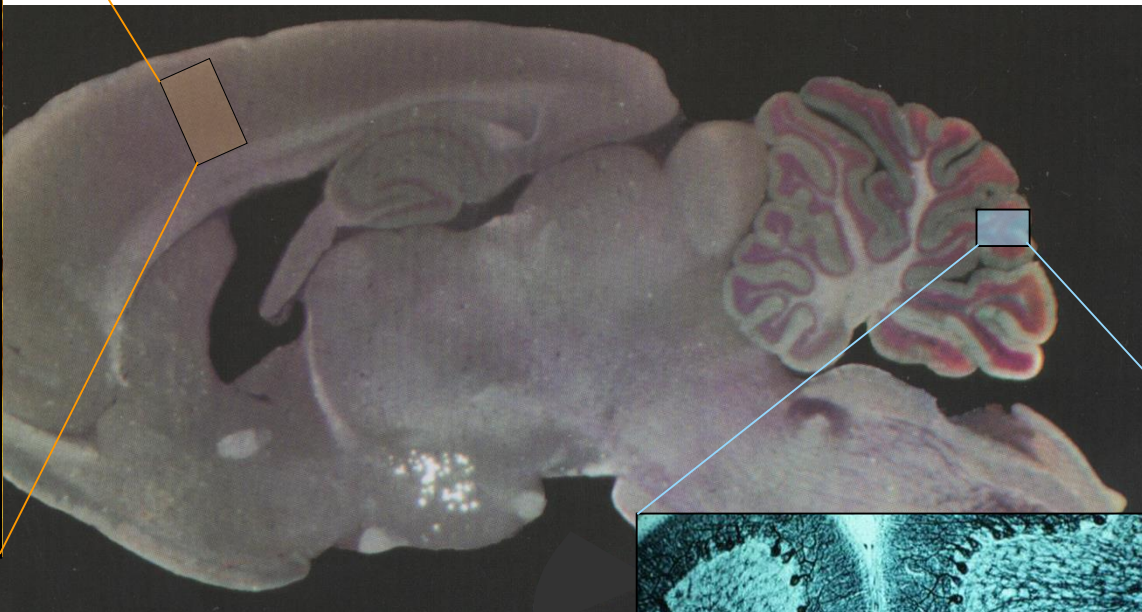
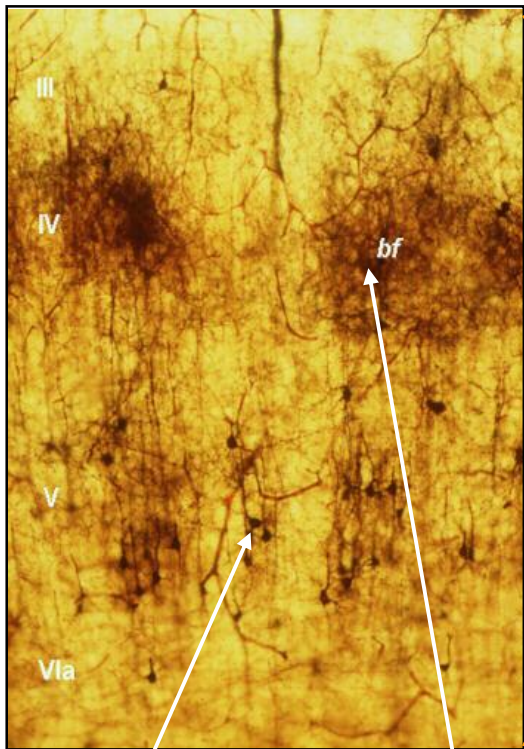


calbindin

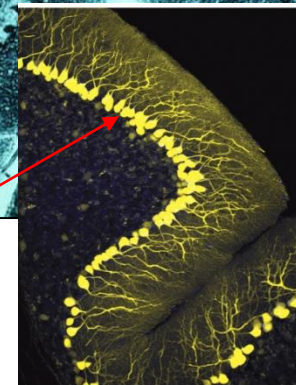


Glutamate transporter  
EAAT4

# Various NEURONAL TYPES in the mammalian brain

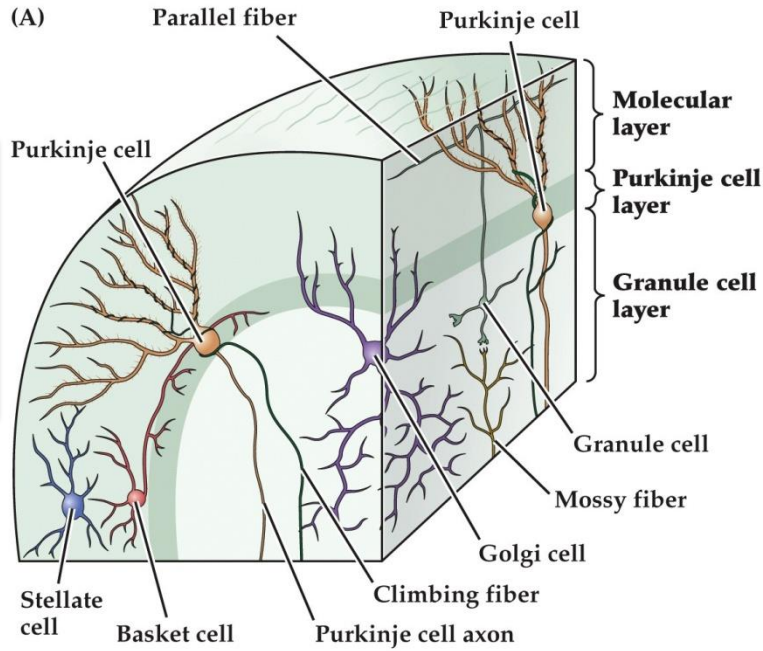


SCIENCE 5e, Figure 19.8 (Part 1)  
Pearson Education, Inc.



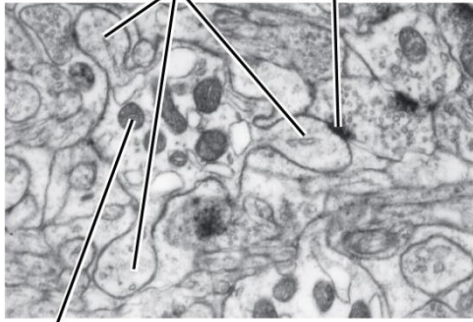
SCIENCE 5e, Figure 19.8 (Part 2)  
Pearson Education, Inc.

# Morphology and neuronal types in the cerebellum

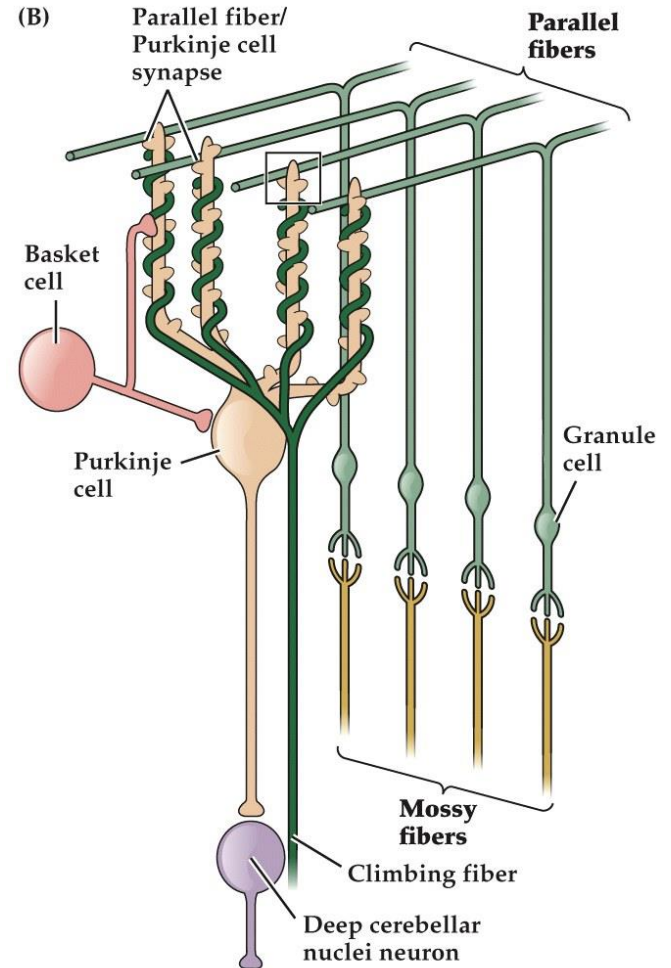


NEUROSCIENCE 5e, Figure 19.9 (Part 1)  
© 2012 Sinauer Associates, Inc.

(C) Spines Parallel fiber synapse



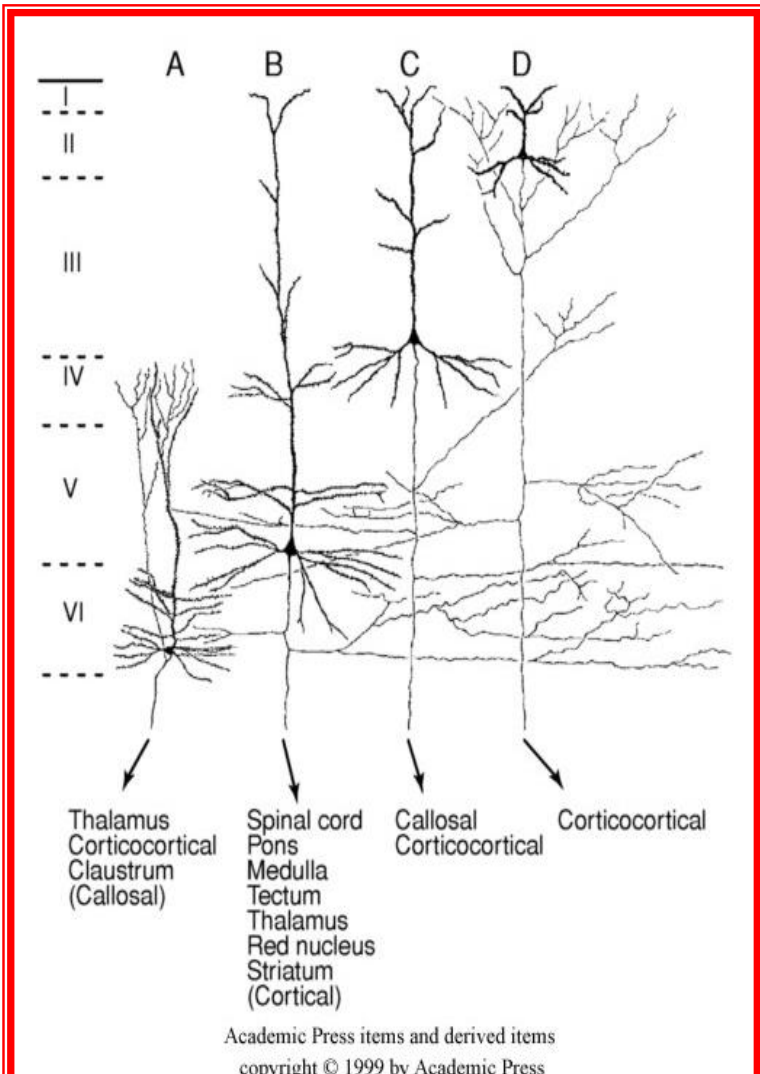
Purkinje cell dendrite



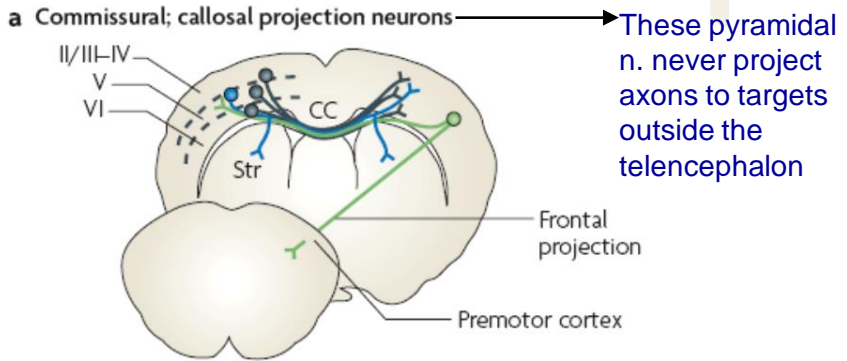
NEUROSCIENCE 5e, Figure 19.9 (Part 2)  
© 2012 Sinauer Associates, Inc.

Molecular/functional heterogeneity of Purkinje cells?

# Morphology and distribution of pyramidal neurons in the neocortex

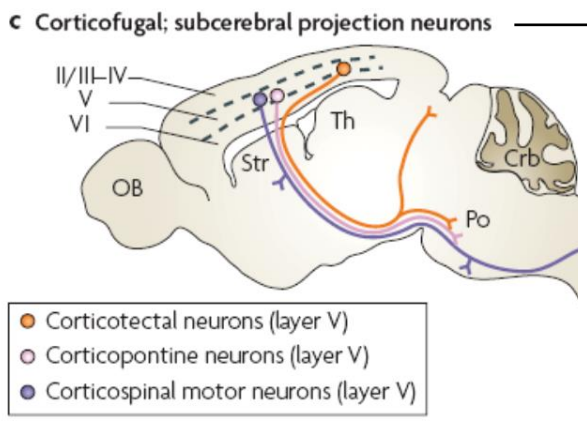
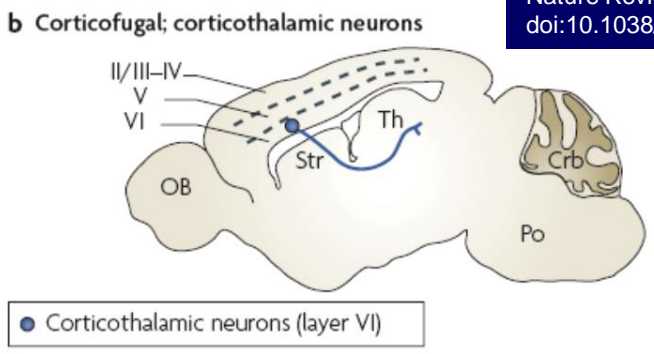


**FIGURE 4** Morphology and distribution of neocortical pyramidal neurons. Note the variability in cell size and dendritic arborization, as well as the presence of axon collaterals, depending on the laminar localization (I–VI) of the neuron. Also, different types of pyramidal neurons with a precise laminar distribution project to different regions of the brain. Adapted from Jones (1984).



These pyramidal n. never project axons to targets outside the telencephalon

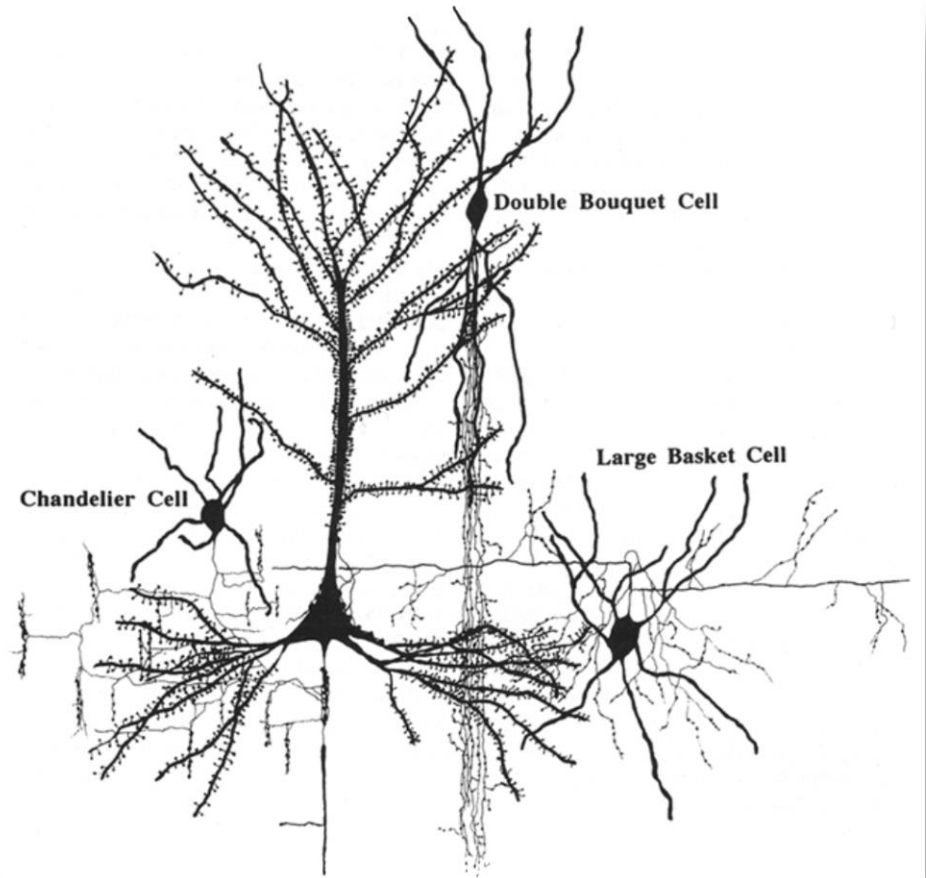
Molyneux et al., 2007  
Nature Reviews Neuroscience  
doi:10.1038/nrn2151



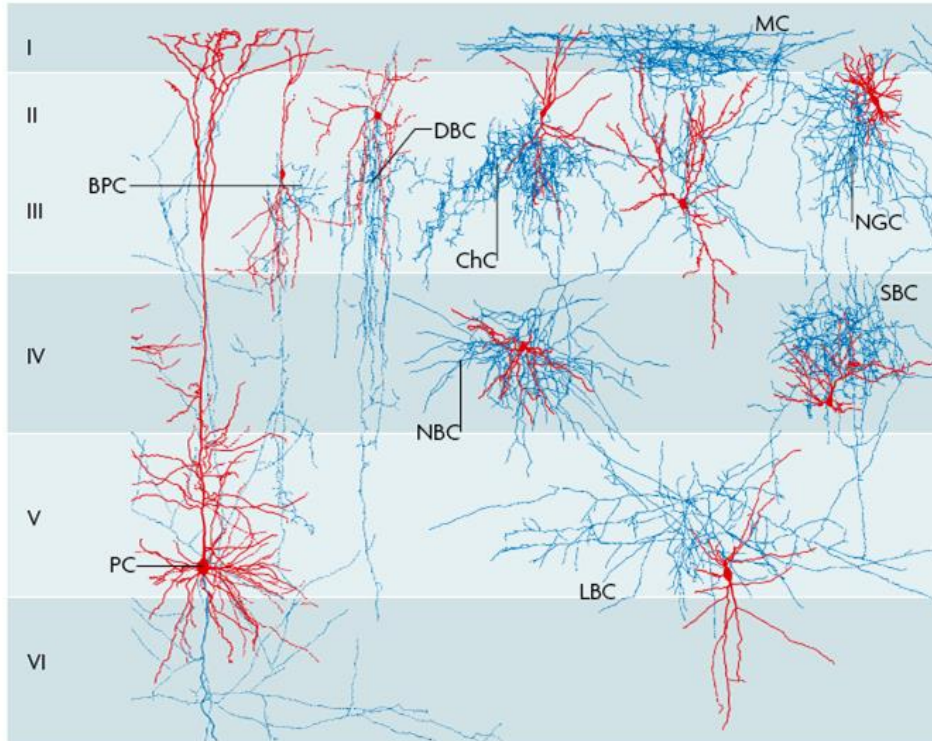
These include Pyramidal neurons of the largest size, which are located in deep-layer V and extend projections to the brainstem and spinal cord

# (Local circuit) cortical interneurons

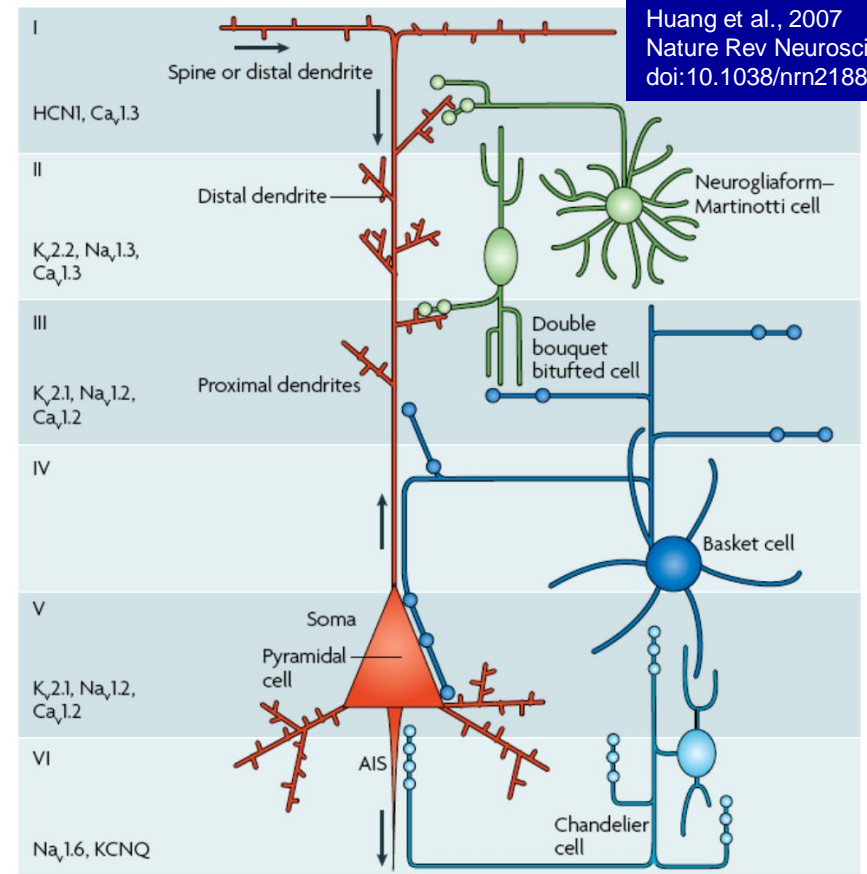
Interneurons comprise 20–30% of the cortical neuronal population and are **locally projecting GABAergic neurons** that control and synchronize the output of pyramidal neurons. Interestingly, the influence of GABAergic interneurons on pyramidal cells is largely dependent on the subcellular location of their inputs, which varies among different interneuron subtypes.



# Neocortical interneurons diversity



**Figure 1 | Axon arbors and innervation patterns of neocortical interneurons.** Interneuron axon arbors distribute inhibitory outputs to discrete spatial domains in the neural network. The figure shows a reconstruction of several classes of neocortical interneurons and, for comparison, a layer five pyramidal neuron (PC; left most). Axons are shown in blue and dendrites are shown in red. The geometry of interneuron axon arbors can be vertical, horizontal, or laminated, suggesting that their output can be distributed to the same or multiple cortical columns, and same or multiple cortical layers. Interneuron axons often elaborate highly exuberant local branches, innervate specific cell types, and impose strong control over local neural populations. Cortical layers are indicated on the left of the figure. BPC, bipolar cell; ChC, chandelier cell; DBC, double bouquet cell; LBC, large basket cell; MC, Martinotti cell; NBC, nested basket cell; NGC, neurogliaform cell; SBC, small basket cell. Images courtesy of Dr Henry Markram (EPFL, Switzerland).



Huang et al., 2007  
Nature Rev Neurosci  
doi:10.1038/nrn2188

**Figure 2 | The subcellular organization of GABAergic inputs.** Pyramidal neurons (shown in red) in the neocortex are characterized by their large size, striking polarity and distinct subcellular domains. The compartmentalized forward and backward electrical signalling (depicted by arrows) arises from the targeted distribution of signalling mechanisms, receptors and ion channels. The distributions of several voltage-gated sodium ( $\text{Na}_v$ ), potassium ( $\text{K}_v$ ; KCNQ) and calcium ( $\text{Ca}_v$ ) channels, and of a hyperpolarization-activated cyclic nucleotide-gated (HCN) cation channel are highlighted to the left of the pyramidal neuron. The subcellular organization of different classes of GABAergic inhibitory inputs is superimposed on the anatomical and physiological compartments of pyramidal neurons, allowing effective regulation of synaptic integration, spike generation, back propagation and plasticity. The stereotyped position and geometry of pyramidal neurons within a cortical column (cortical layers are indicated on the left) suggests that their subcellular architecture significantly affects neuronal signalling in cortical circuits. AIS, axon initial segment; GABA,  $\gamma$ -aminobutyric acid. Modified, with permission, from *Nature Rev. Neurosci.* REF. 27 © (2005) Macmillan Publishers Ltd.

# “Easy” neuronal classification

## **Structural classification:**

Unipolar, bipolar, multipolar, more ...

## **Functional classification:**

- **projection** (inter)neurons
- local circuit **interneurons**
  
- **excitatory** (neurotransmitters: Glutamate, etc.)
- **inhibitory** (neurotransm.: GABA, glycine, etc.)

**This classification is not sufficient to describe neuronal diversity!**



# The problem of neuronal classification and subtype identification.....

We need to classify different neuronal types in order to speak a “common language” with other neuroscientists and in order to understand the complexity of brain function...

**HOW should we classify neurons?**

**By morphology?**

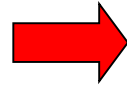
**By functional features?**

**By expression markers?**

**How do we put together information from different approaches?**

for discussion see [Yuste, 2005](#)

# The problem of neuronal classification...



The obvious (but not the easiest) solution would be COMBINING different approaches in the same experimental model. An example:

## Localization of Calcium-binding Proteins in Physiologically and Morphologically Characterized Interneurons of Monkey Dorsolateral Prefrontal Cortex

A.V. Zaitsev<sup>1</sup>, G. Gonzalez-Burgos<sup>1</sup>, N.V. Povysheva<sup>1</sup>, S. Kröner<sup>2,3</sup>, D.A. Lewis<sup>1,2</sup> and L.S. Krimer<sup>1</sup>

Cerebral Cortex August 2005;15:1178-1186

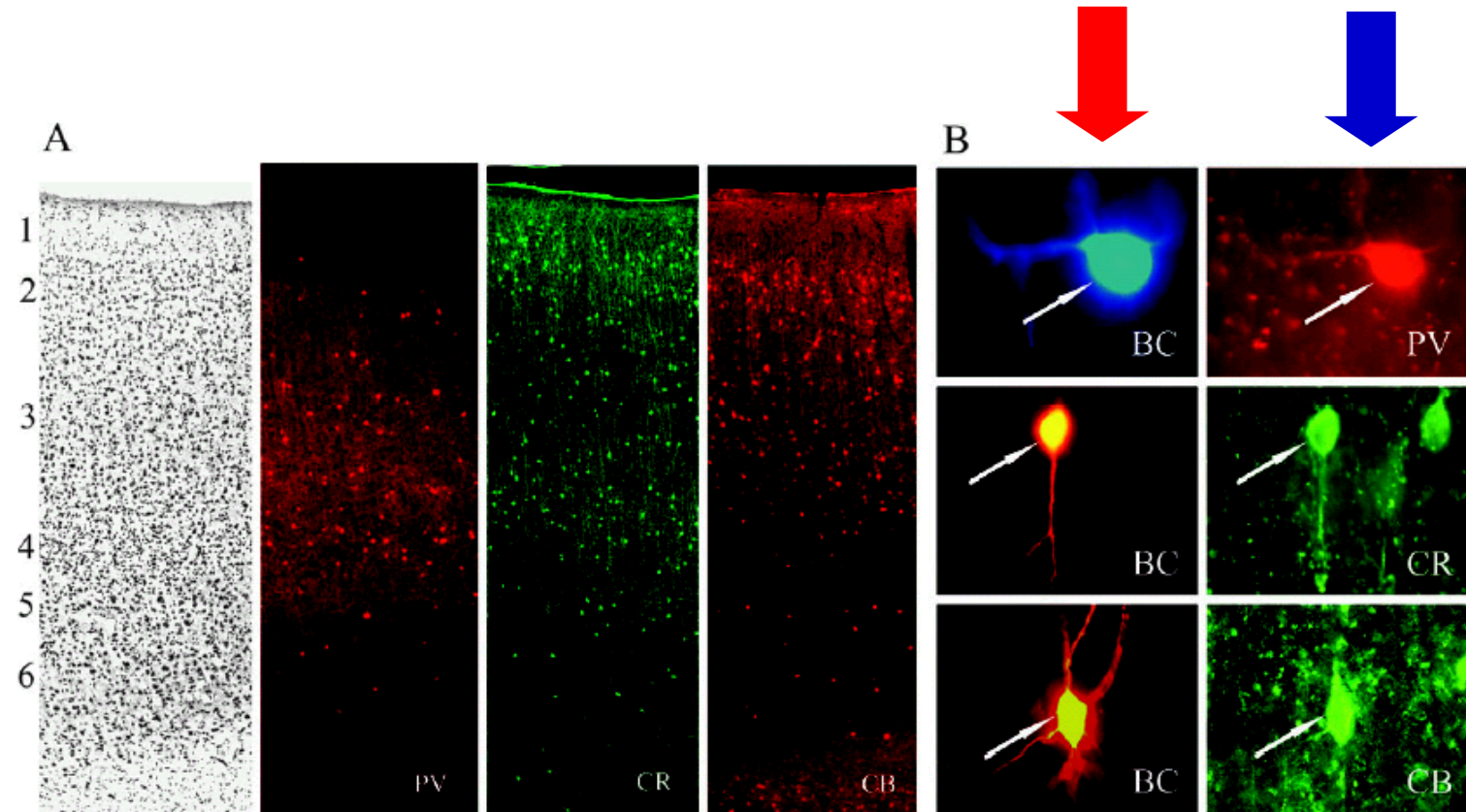
### ABSTRACT

In the primate neocortex, little is known about the possible associations between functional subclasses of GABA neurons, their morphological properties and calcium-binding protein (CaBP) content. We used whole-cell current clamp recordings, combined with intracellular labeling and fluorescence immunohistochemistry, to determine these relationships for interneurons in layers 2-3 of monkey prefrontal cortex (PFC). Eighty-one interneurons were included in the analysis. Thirty-eight of these cells showed immunoreactivity for one of the three CaBPs tested. Co-localization of more than one CaBP was not observed in any of the interneurons examined. Interneurons with different CaBPs formed distinct populations with specific physiological membrane properties and morphological features. Parvalbumin (PV)-positive cells had the physiological properties characteristic of fast-spiking interneurons (FS) and the morphology of basket or chandelier neurons. Most calretinin (CR)-containing cells had the physiological properties ascribed to non-fast-spiking cells (non-FS) and a vertically oriented axonal morphology, similar to that of double bouquet cells. Calbindin (CB)-positive interneurons also had non-FS properties and included cells with double bouquet morphology or with a characteristic dense web of axonal collaterals in layer 1. Classification of the interneurons based on cluster analysis of multiple electrophysiological properties suggested the existence of at least two distinct groups of interneurons. The first group contained mainly PV-positive FS cells and the second group consisted predominantly of CR- and CB-positive non-FS interneurons. These findings may help to illuminate the functional roles of different groups of interneurons in primate PFC circuitry.

- (1) Whole-cell electrophysiological recording on cortical slices
- +
- (2) intracellular injection of biocytin in recorded neurons (for later recognition and morphological analysis)
- +
- (3) fluorescence immunocytochemistry for selected markers (calcium-binding proteins: parvalbumin, calbindin and calretinin)

# The phenotype of **BC-injected/electrophysiologically-recorded** interneurons is determined by **immunocytochemistry**

Zaitsev et al., 2005  
Cerebral Cortex  
doi:10.1093/cercor/bhh218



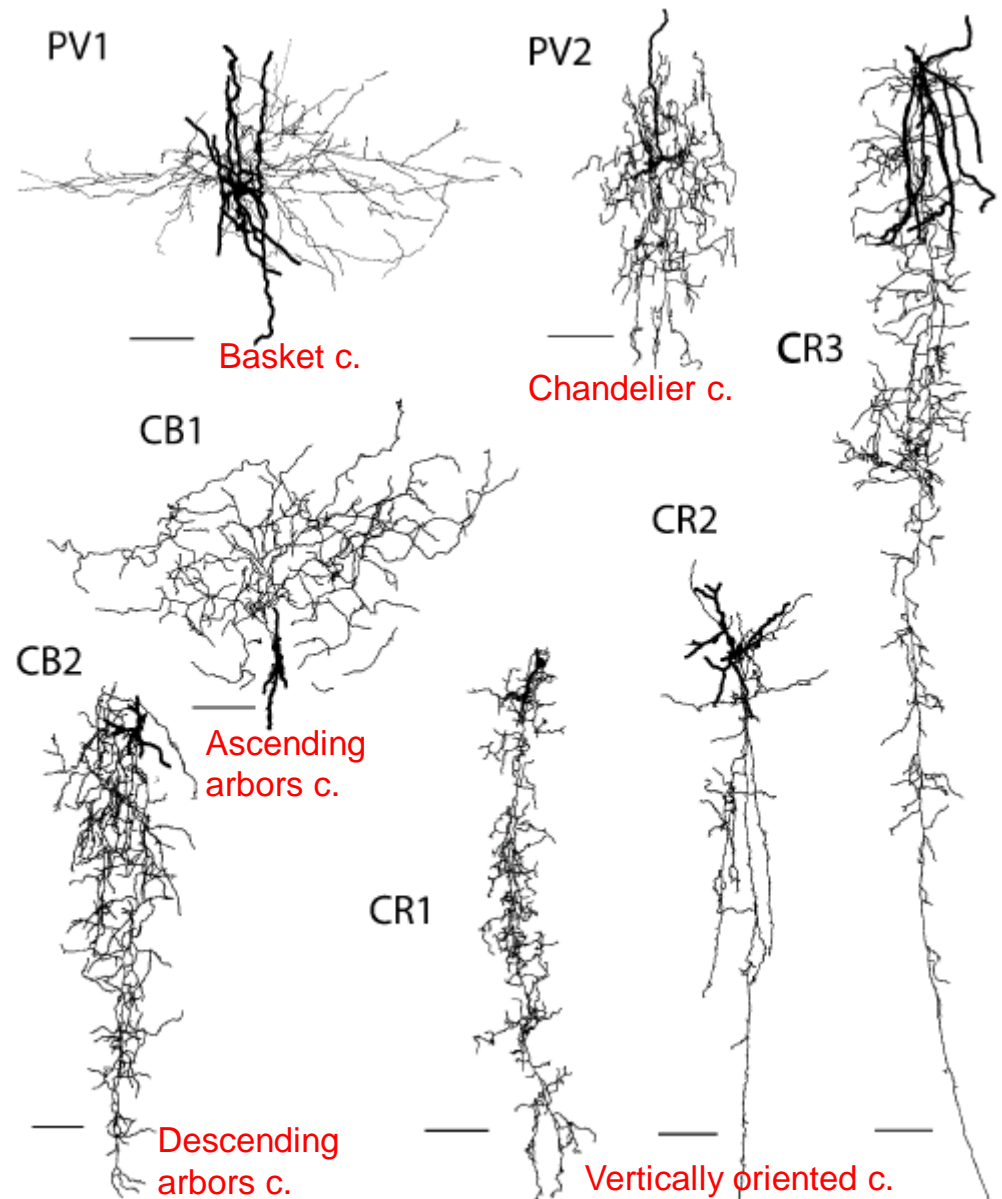
**Figure 1.** Fluorescence-labeling of CaBPs in monkey DLPFC interneurons. (A) Photomicrographs of adjacent coronal sections (area 46) with laminar boundaries; from left Nissl stain, PV-, CR- and CB-IR structures. Note the substantial differences in the laminar distribution of the neurons labeled for each CaBP. (B) Dual-label photomicrographs from the same microscopic field, showing immunohistochemical identification of physiologically characterized biocytin (BC)-injected interneurons as positive for PV, CR or CB. Arrows show the cell bodies. Top: BC visualized by streptavidin-Alexa Fluor<sup>®</sup> 350 conjugate (blue), PV-IR visualized by Alexa Fluor<sup>®</sup> 594 conjugated secondary antibody. Middle: BC visualized by streptavidin-Alexa Fluor<sup>®</sup> 568 conjugate, CR-IR visualized by Alexa Fluor<sup>®</sup> 488 conjugated secondary antibody. Bottom: BC visualized by streptavidin-Alexa Fluor<sup>®</sup> 568 conjugate, CB-IR visualized by Alexa Fluor<sup>®</sup> 488 conjugated secondary antibody.



<https://www.jove.com/science-education/5040/introduction-to-fluorescence-microscopy>

The combination of intracellular-injection techniques and immunocytochemistry suggests that the same phenotypic marker is expressed by interneurons with different morphologies

Do different morphologies indicate different functional features?

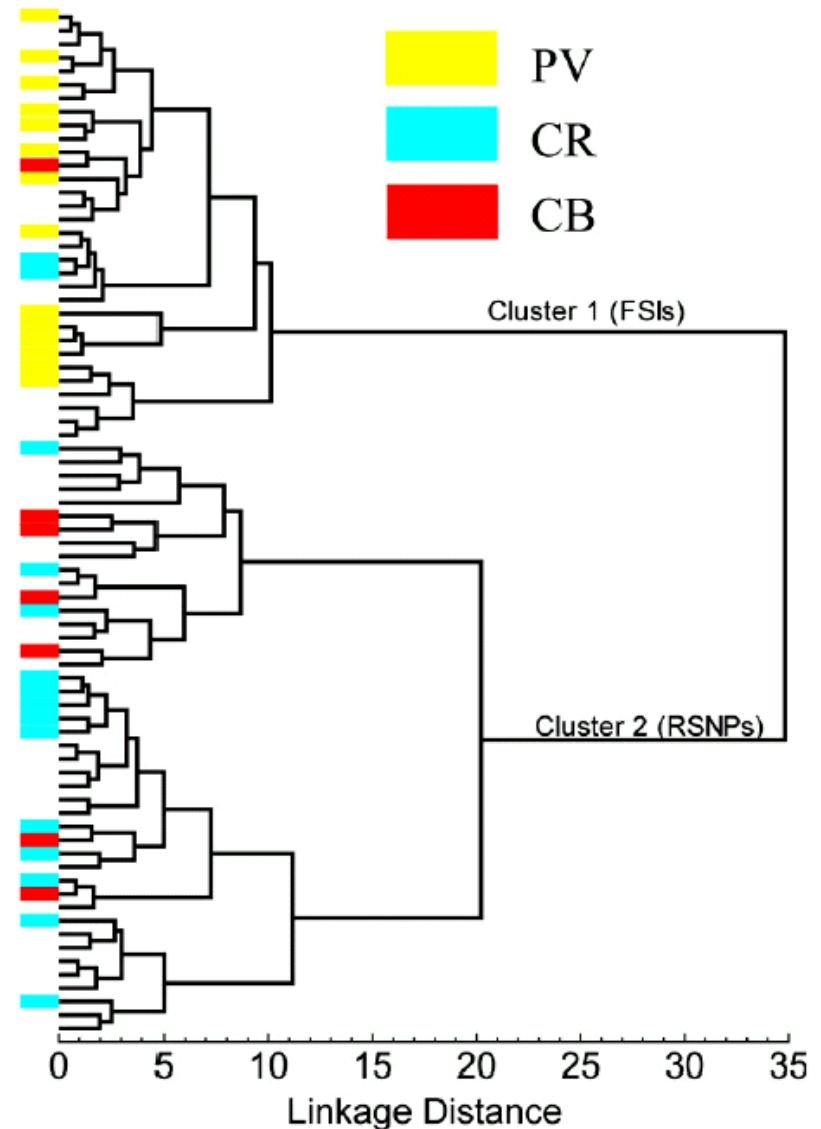


**Figure 2.** Three-dimensional reconstructions of biocytin-labeled interneurons from monkey DLPFC. PV1, PV-IR spreading arbor (basket) cell; PV2, PV-IR chandelier cell; CR1-CR3, examples of CR-IR vertically oriented cells; CB1, CB-IR cell with ascending arbors; CB2, CB-IR cell with descending arbors. Calibration bars = 100  $\mu$ m.

Data were processed using **CLUSTER ANALYSIS:** correlation between **electrophysiological properties** and **expression of specific Ca<sup>+</sup>-binding proteins**

When cells are grouped based only on electrophysiological properties, two main groups (= clusters) of interneurons are obtained: FS (Fast Spiking) and non-FS.

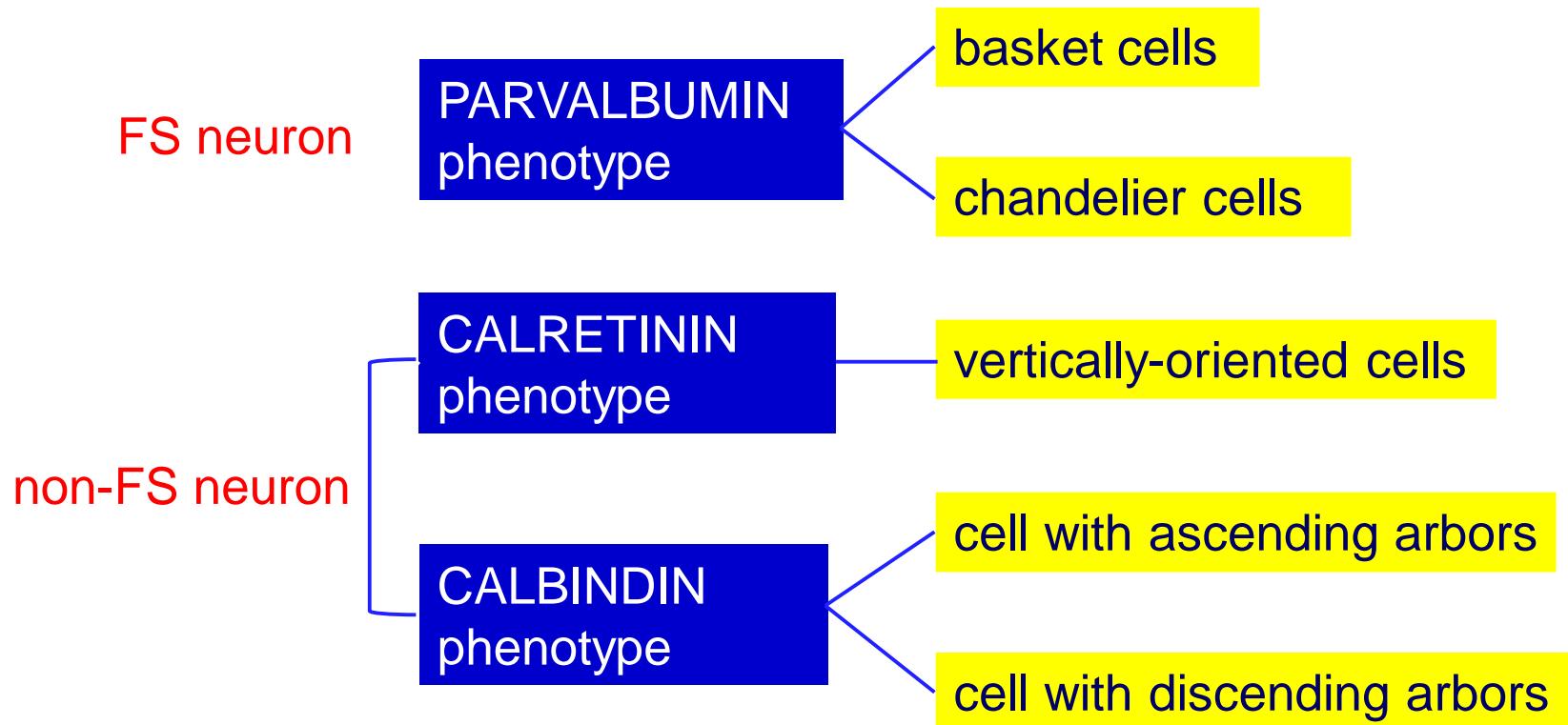
These two clusters do show significant differences in Ca<sup>+</sup>-binding protein content



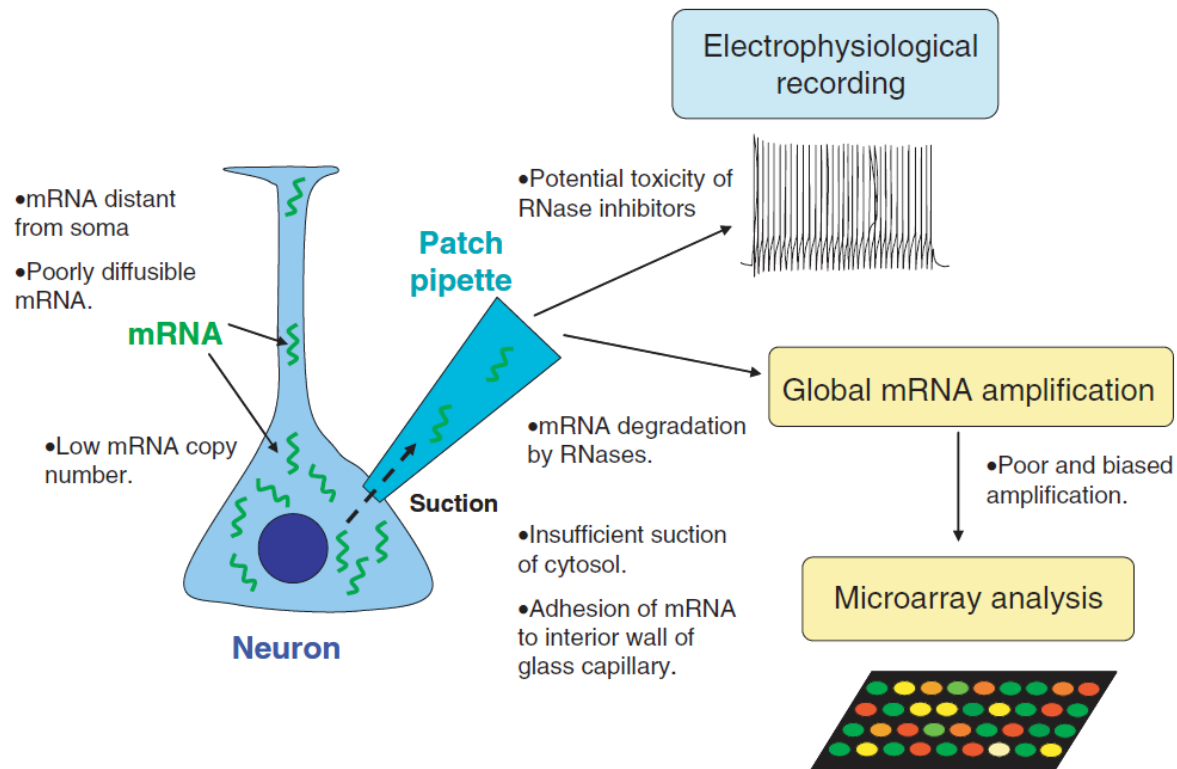
**Figure 4.** Hierarchical tree plot illustrating the results of cluster analysis. There are two main branches corresponding to FS interneurons (FSI) and non-FS cells. The first cluster mainly contained PV-positive interneurons and the second one consisted exclusively of CB- and CR-positive cells.

## CONCLUSIONS:

- parvalbumin-expressing interneurons are exclusively FS
- calretinin- and calbindin-expressing interneurons are mainly non-FS
- multiple morphologies can correspond to a single functionally-defined phenotype



# Electrophysiological and gene expression profiling of neuronal cell types



**Figure 1. Potential problems with single-cell gene expression profiling by cytoplasmic harvesting via patch-pipette**

Collecting extremely low amounts of mRNA from single cells is the biggest challenge of this technique. Only a small proportion of cytosol can be obtained by suction via patch-pipette, and poorly diffusible mRNA or dendritic mRNA are particularly hard to collect. The yield of mRNA can be improved by including inhibitors of RNases in the pipette, but these are often cytotoxic and can be detrimental to electrophysiological recording. It is also possible that some mRNA adheres to the interior wall of the glass capillary and evades expulsion from the patch-pipette.

another way to classify cortical interneurons is....

....to consider their **developmental origin:**

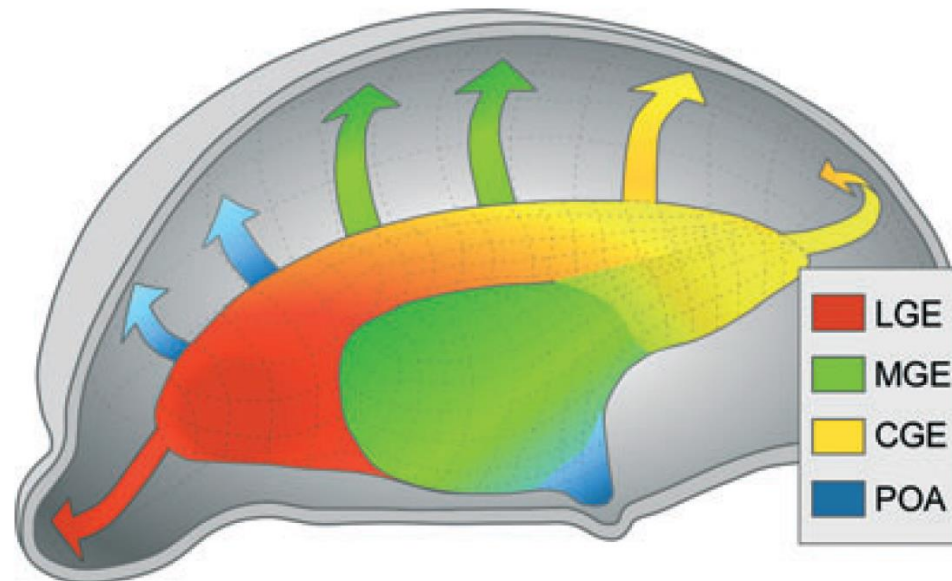
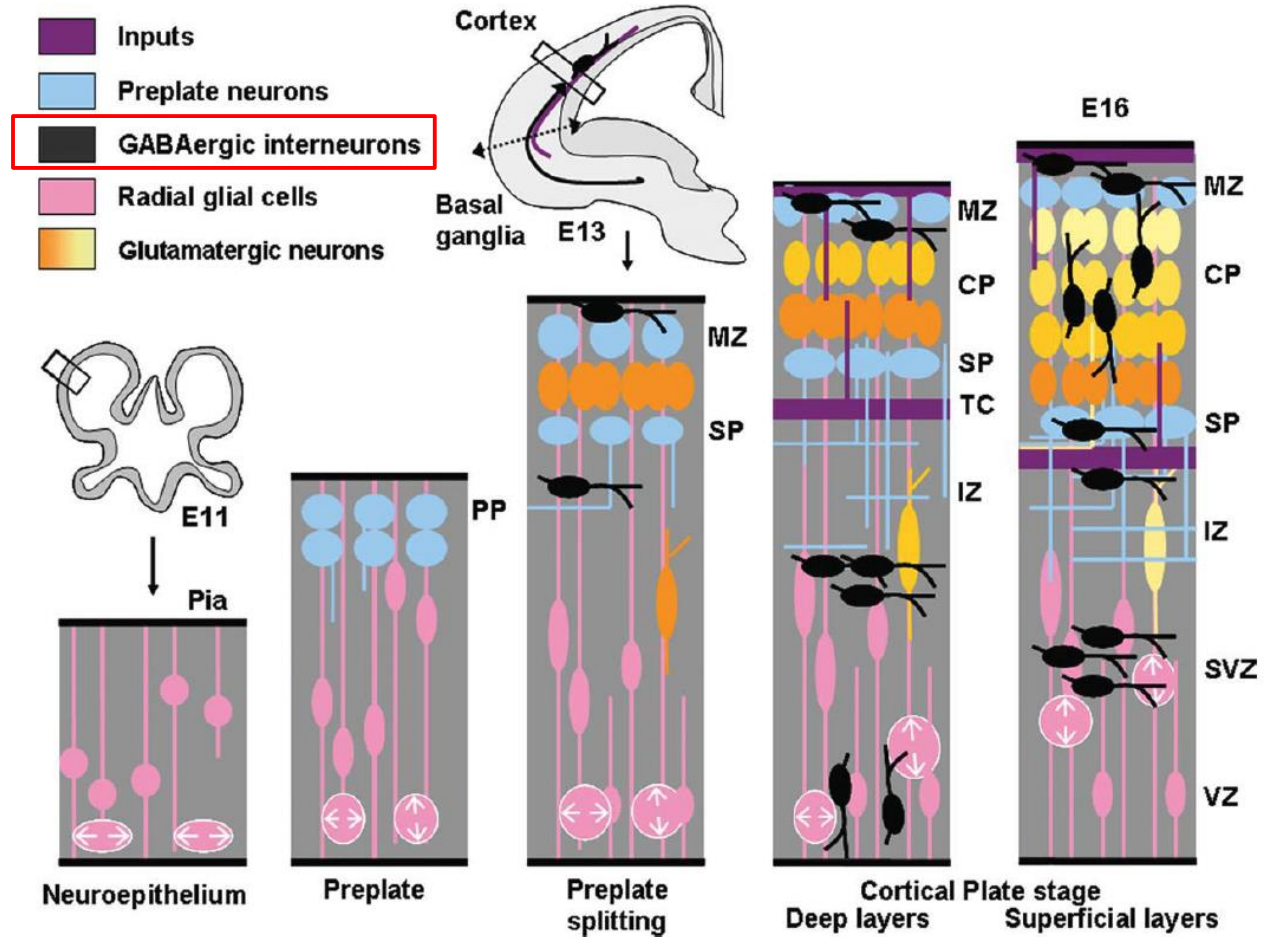


FIG. 2. Cortical interneurons are born in the subpallium and migrate tangentially to the cortex. The schema represents an E13.5 embryo brain hemisection. The arrows show representative migratory routes.

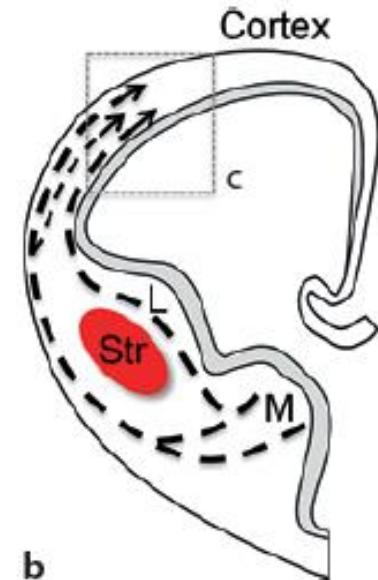
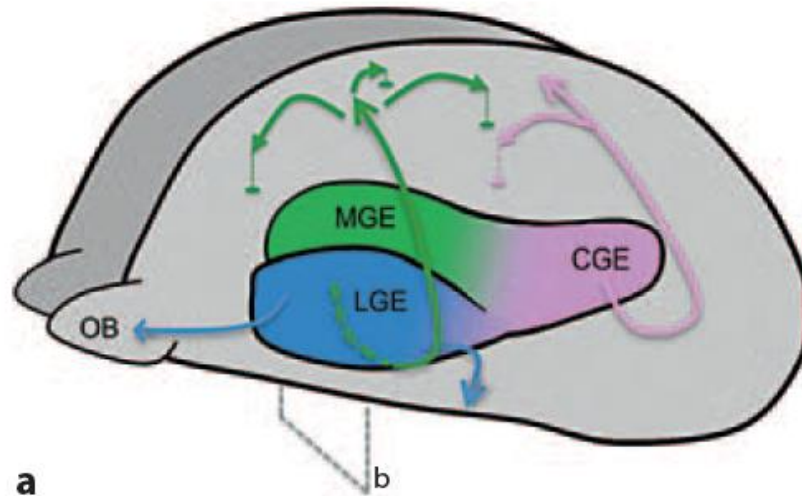


# Cortical development



**Figure 1** Cortical development. Schematic drawings of coronal sections of the developing mouse cortex. Afferent axons and the migration of telencephalic interneurons from the basal telencephalon are drawn in purple and black respectively. Cortical development begins with the appearance of a population of cells along the lateral ventricle, known as the ventricular zone (E11; VZ). This population of cells gives rise to most of the neurons and glial cells of the cerebral cortex. Once generated, neurons migrate towards the pial surface and complete their differentiation in the cortical plate. Neurons that will populate the deeper layers of the cortex are generated and then migrate away from the VZ earlier than the neurons that will populate progressively more superficial layers. On E12-E13, the cerebral wall is bilaminar consisting of the VZ and overlying primitive preplate. By E17-E18 the thickness of the overlying intermediate zone/with matter and developing cortical plate are at their maximum widths, with all neuronal cells having exited the cell cycle and migrated to their final laminar distribution within the developing cortex. CP, cortical plate; IZ, intermediate zone; MZ, marginal zone; PP, preplate; SP, subplate; TC, thalamocortical axons; SVZ, subventricular zone.

# Primary routes of interneuron migration during cortical development.



**Cortical interneurons** born in the MGE and CGE in the ventral telencephalon follow tangential migratory paths into the developing cortex. Once within the cortical wall, cells disperse before entering the cortical plate and reside in a final position. The LGE-derived neurons migrate rostrally and ventrally into the olfactory bulb (OB) and striatum, respectively

Coronal section (indicated in a) illustrating the major routes of tangential migration through the embryonic telencephalon. Interneurons migrate from the MGE (M) and traverse the LGE (L) whilst avoiding the striatum (Str).

## The Temporal and Spatial Origins of Cortical Interneurons Predict Their Physiological Subtype

Simon J.B. Butt,<sup>1,3</sup> Marc Fuccillo,<sup>1,3</sup> Susana Nery,<sup>1,4</sup>  
Steven Noctor,<sup>2,5</sup> Arnold Kriegstein,<sup>2,5</sup>  
Joshua G. Corbin,<sup>1,6</sup> and Gord Fishell<sup>1,\*</sup>

MGE-originating  
interneurons

**FS**,  
parvalbumin(somato  
statin)-positive cells

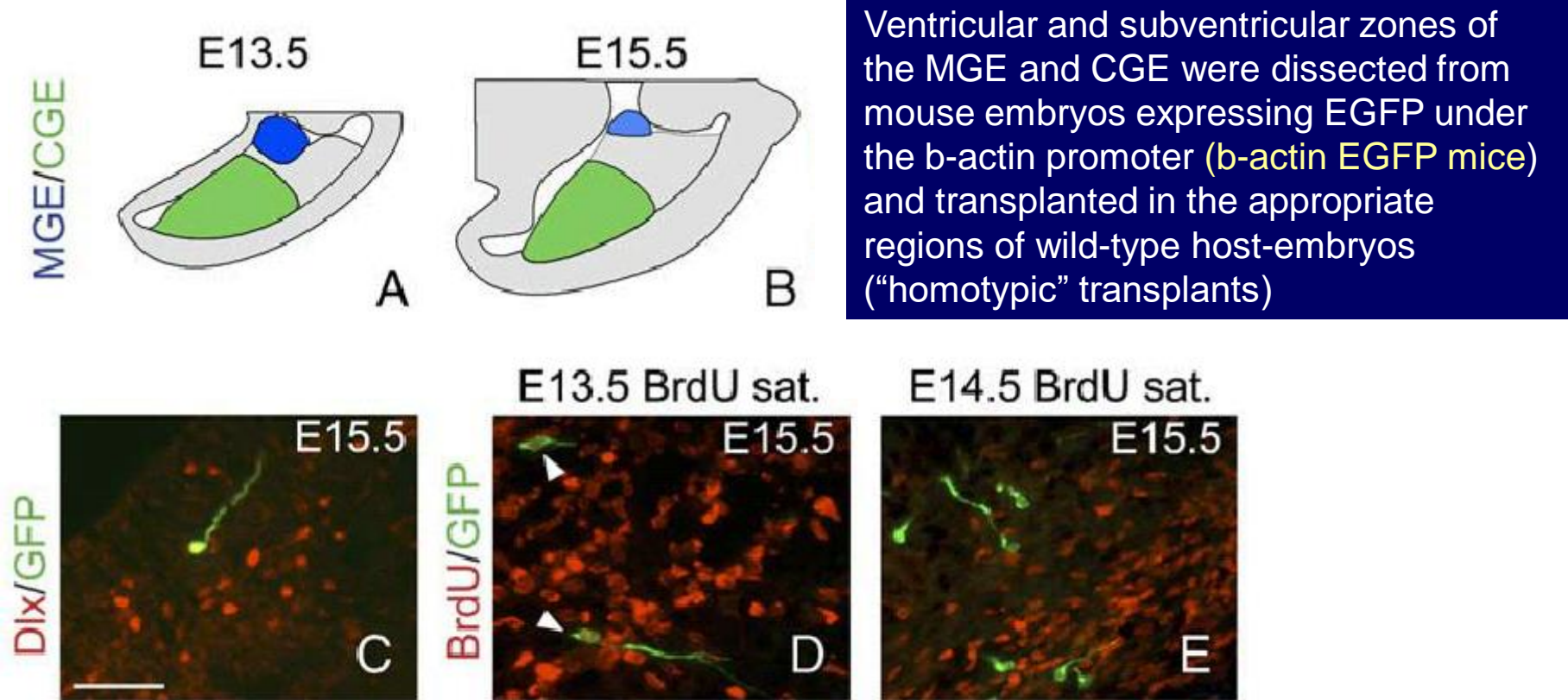
CGE-originating  
interneurons

**non-FS**,  
calretinin(VIP, NPY)-  
positive cells

### Summary

Interneurons of the cerebral cortex represent a heterogeneous population of cells with important roles in network function. At present, little is known about how these neurons are specified in the developing telencephalon. To explore whether this diversity is established in the early progenitor populations, we conducted in utero fate-mapping of the mouse medial and caudal ganglionic eminences (MGE and CGE, respectively), from which most cortical interneurons arise. Mature interneuron subtypes were assessed by electrophysiological and immunological analysis, as well as by morphological reconstruction. At E13.5, the MGE gives rise to fast-spiking (FS) interneurons, whereas the CGE generates predominantly regular-spiking interneurons (RSNP). Later at E15.5, the CGE produces RSNP classes distinct from those generated from the E13.5 CGE. Thus, we provide evidence that the spatial and temporal origin of interneuron precursors in the developing telencephalic eminences predicts the intrinsic physiological properties of mature interneurons.

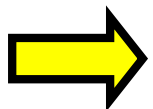
# In utero fate-mapping of cortical interneurons ...



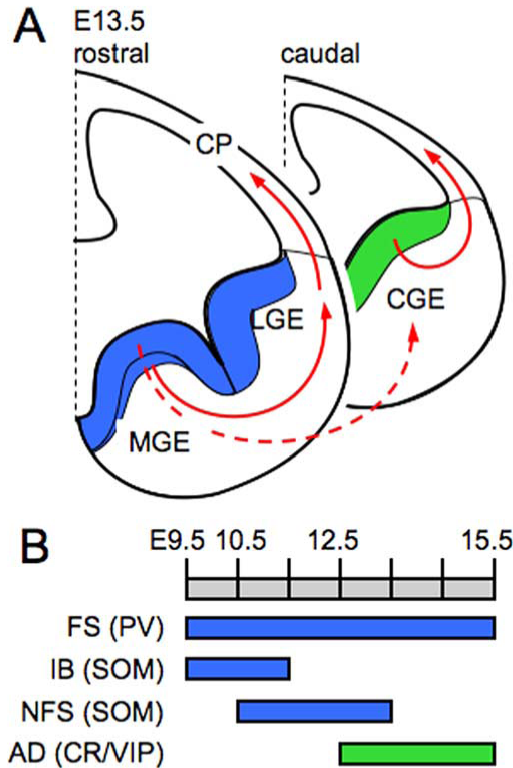
Ventricular and subventricular zones of the MGE and CGE were dissected from mouse embryos expressing EGFP under the b-actin promoter (b-actin EGFP mice) and transplanted in the appropriate regions of wild-type host-embryos ("homotypic" transplants)

Figure 1. In Utero Fate-Mapping of the Ventral Telencephalic Eminences

(A and B) Schematic of the regions taken from the ventral telencephalon for in utero transplantation, as seen with the cortex removed and viewed from above. (C) Many transplanted progenitors expressed Dlx proteins, a characteristic of developing interneurons. BrdU saturation was performed immediately after transplantation (D) and 1 day following transplantation of MGE progenitors at E13.5 (E). Embryos sacrificed at E15.5 and stained with BrdU and GFP showed that while many progenitors proliferated immediately after transplantation (white arrowheads), after 1 day there were fewer proliferative transplanted neurons (E).



# electrophysiological, immunocytochemical and morphological reconstruction of mature interneurons in young-adult mice



**Figure 1.** Subcortical origins of cortical interneurons in the mouse telencephalon. *A*, Diagram showing rostral and caudal coronal sections through an embryonic (embryonic day 13.5 (E13.5)) mouse telencephalon. The large majority of cortical interneurons originate from the proliferative zone (PZ) (the ventricular and subventricular zones) of two subcortical structures, the MGE (blue PZ) and CGE (green PZ), before migrating tangentially (filled red arrows) into the developing cortical plate (CP). Transplantation experiments suggest that interneurons from the MGE also migrate caudally (dashed red arrow) via the CGE before undergoing tangential migration. *B*, Evidence from both transplantation and genetic fate-mapping experiments has revealed distinct spatial and temporal origins for distinct physiological subtypes of interneuron as assayed by their intrinsic properties. The bulk of interneuron neurogenesis occurs from E9.5 until E15.5 (gray scale bar). Fast spiking interneurons, most of which express PV, burst spiking interneurons (IB), most of which express SOM, and SOM-positive nonfast spiking interneurons (NFS) originate from the MGE with different temporal profiles (blue histogram bars). Adapting (AD) interneurons, which primarily express CR and/or vasoactive intestinal peptide (VIP), originate at later time points from the CGE (green bar).

## CONCLUSIONS:

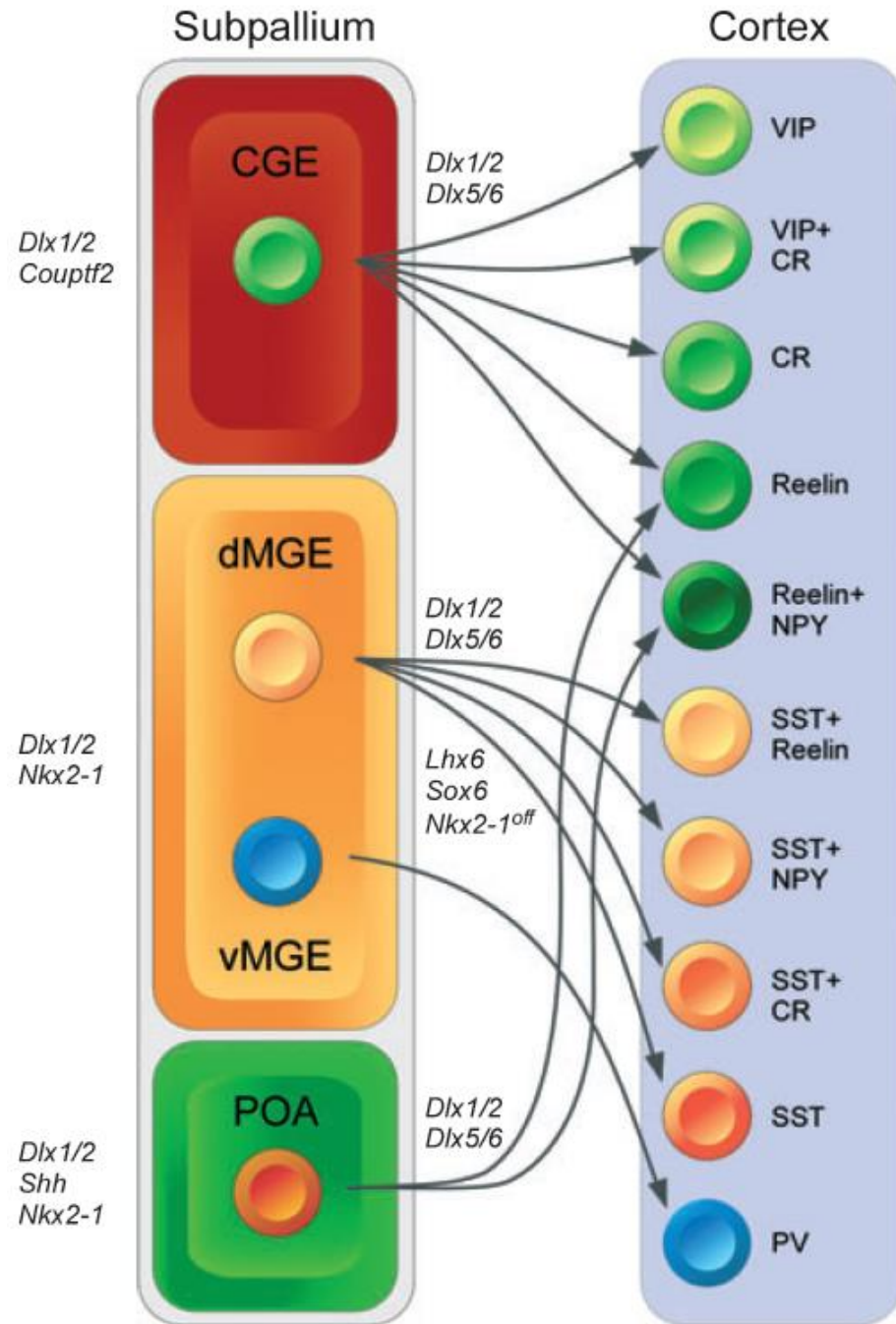
- parvalbumin-expressing/FS/basket-shaped neurons originate from MGE
- calretinin-expressing/non-FS/bipolar (vertically-oriented?) neurons originate from CGE

This means that different subtypes of interneurons are generated at different spatial positions (= from different progenitors)

**CLASSIFYING** neurons **BY THEIR ORIGIN** could be a new method of neuronal classification

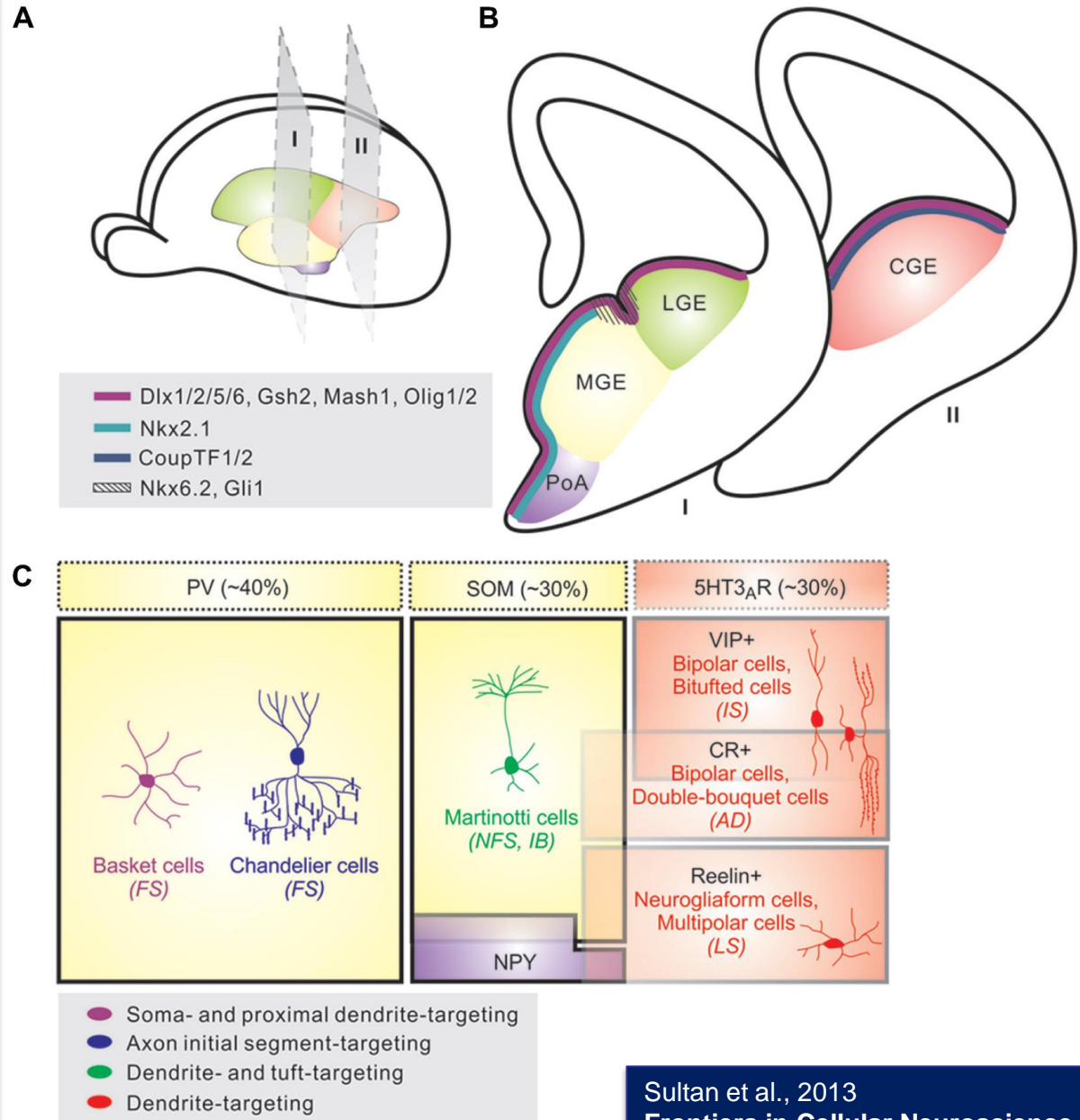
## Cortical interneuron diversity largely emerges from spatially segregated progenitor cells with distinct transcriptional profiles

FIG. 3. Cortical interneuron diversity largely emerges from spatially segregated progenitor cells with distinct transcriptional profiles. The schema shows the main sources of cortical interneurons, CGE, MGE and POA, which contain progenitor cells that can be distinguished by their expression of transcription factors and other proteins. Thus, CGE cells express both *Dlx1/2* and *Couptf2*, MGE cells express *Dlx1/2* and *Nkx2-1*, and POA cells express *Dlx1/2*, *Nkx2-1* and *Shh*. Furthermore, each of these regions seems to contain distinct progenitor domains (not shown in the schema), characterized by the expression of different transcription factors (Flames *et al.*, 2007). Each progenitor region produces a particular group of interneurons, although some interneuron classes may emerge from different progenitor domains. This is the case for multipolar reelin/NPY-containing interneurons, which derive from both CGE and POA. It is possible, however, that these cells derive from a progenitor domain that bridges the two structures and that is characterized by the expression of *Couptf2* (Kanatani *et al.*, 2008). Only the mechanisms involved in the generation of MGE cells are beginning to be elucidated. Thus, down-regulation of *Nkx2-1* and expression of *Lhx6* and *Sox6* are necessary for the proper specification of MGE-derived interneurons.



## IN SUMMARY: Origins and diversity of neocortical interneurons

**(A)** Neocortical interneurons are derived from progenitor cells located in the proliferative zones of the ventral telencephalon, specifically within the medial ganglionic eminence (MGE) and caudal ganglionic eminence (CGE). A small proportion is produced in the preoptic area (PoA). **(B)** Various transcription factors are expressed in distinct patterns throughout the subpallial germinal zones. **(C)** Neocortical interneurons are highly diverse and can be defined based on morphology, neurochemical expression, electrophysiological properties, and subcellular synaptic targeting specificity.

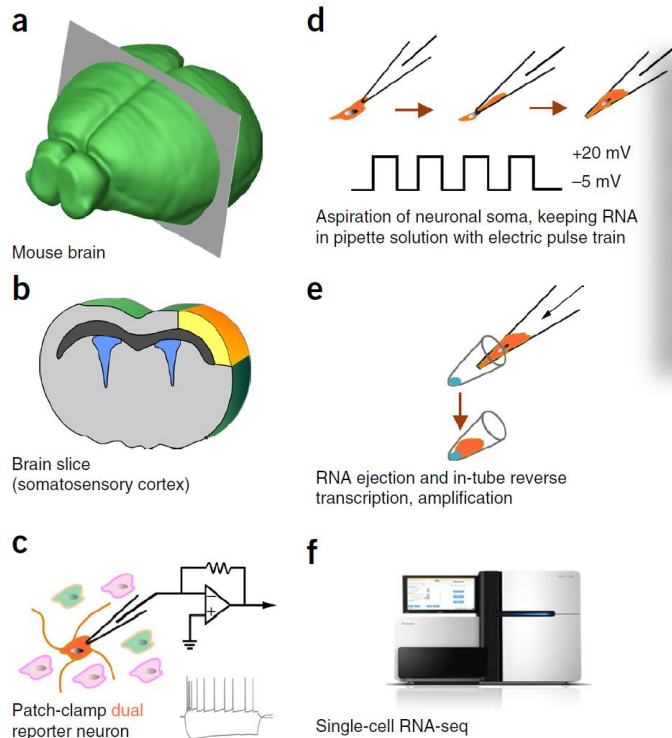


# Integration of electrophysiological recordings with single-cell RNA-seq data identifies neuronal subtypes

János Fuzik<sup>1,2,5</sup>, Amit Zeisel<sup>1,5</sup>, Zoltán Máté<sup>3</sup>, Daniela Calvigioni<sup>1,2</sup>, Yuchio Yanagawa<sup>4</sup>, Gábor Szabó<sup>3</sup>, Sten Linnarsson<sup>1,6</sup> & Tibor Harkany<sup>1,2,6</sup>

Fuzik et al., 2016  
Nature Biotech  
doi:10.1038/nbt.3443

Traditionally, neuroscientists have defined the identity of neurons by the cells' location, morphology, connectivity and excitability. However, the direct relationship between these parameters and the molecular phenotypes has remained largely unexplored. Here, we present a method for obtaining full transcriptome data from single neocortical pyramidal cells and interneurons after whole-cell patch-clamp recordings in mouse brain slices. In our approach, termed Patch-seq, a patch-clamp stimulus protocol is followed by the aspiration of the entire somatic compartment into the recording pipette, reverse transcription of RNA including addition of unique molecular identifiers, cDNA amplification, Illumina library preparation and sequencing. We show that Patch-seq reveals a close link between electrophysiological characteristics, responses to acute chemical challenges and RNA expression of neurotransmitter receptors and channels. Moreover, it distinguishes neuronal subpopulations that correspond to both well-established and, to our knowledge, hitherto undescribed neuronal subtypes. Our findings demonstrate the ability of Patch-seq to precisely map neuronal subtypes and predict their network contributions in the brain.



## A new way to identify neuronal subtypes with transcriptomics: Patch-seq = patch-clamp + Next Generation Sequencing

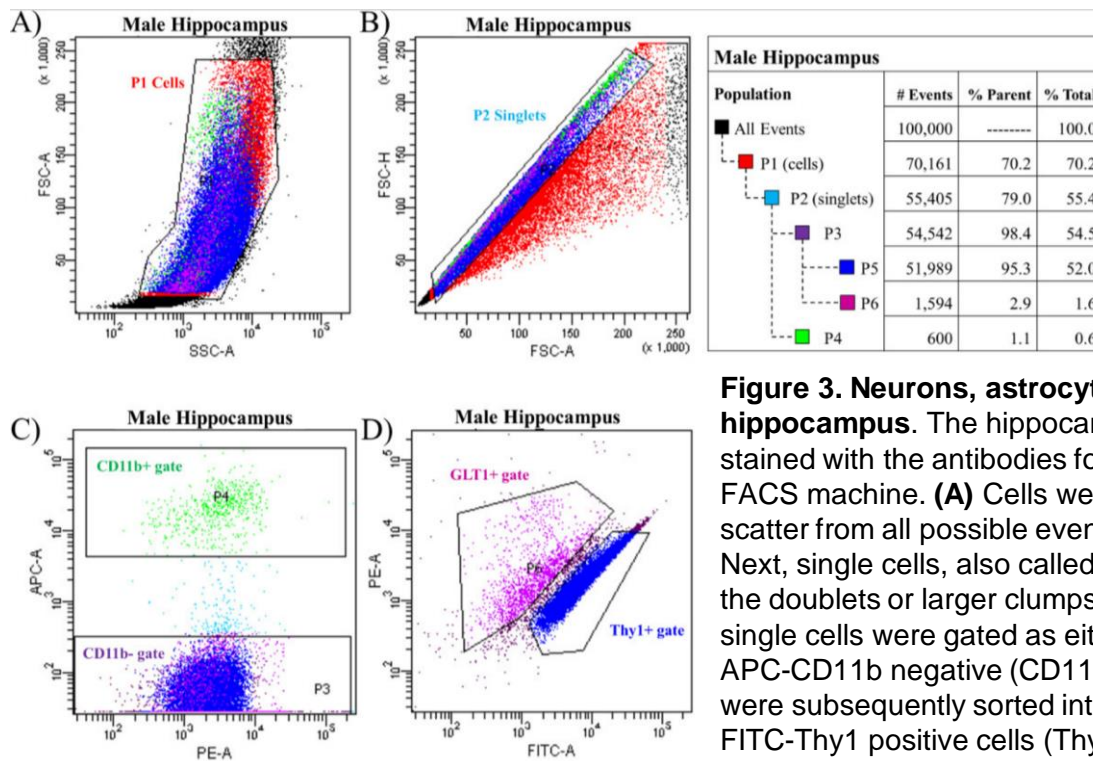
focusing on cholecystokinin (CCK)-containing(+) GABAergic interneurons by using **dual-labeled CCKBAC/dsRed::GAD67gfp/+ mouse reporter**

**Figure 2** Workflow diagram of Patch-seq procedures. (a) Coronal cutting plane of a mouse brain to access the somatosensory cortex. (b) *Ex vivo* brain slice anatomy with the somatosensory cortex highlighted in yellow and orange. (c) Whole-cell patch-clamp recording of DsRed<sup>+</sup>/GFP<sup>+</sup> dual-tagged interneurons. (d) Aspiration of neuronal somata was followed by square voltage pulses from  $-5$  mV (holding potential) to  $+20$  mV, while maintaining negative pressure. (e) The sample was expelled into lysis buffer, which allowed for in-tube reverse transcription by PCR. (f) Single-cell RNA sequencing performed on an Illumina HiSeq2000 instrument.

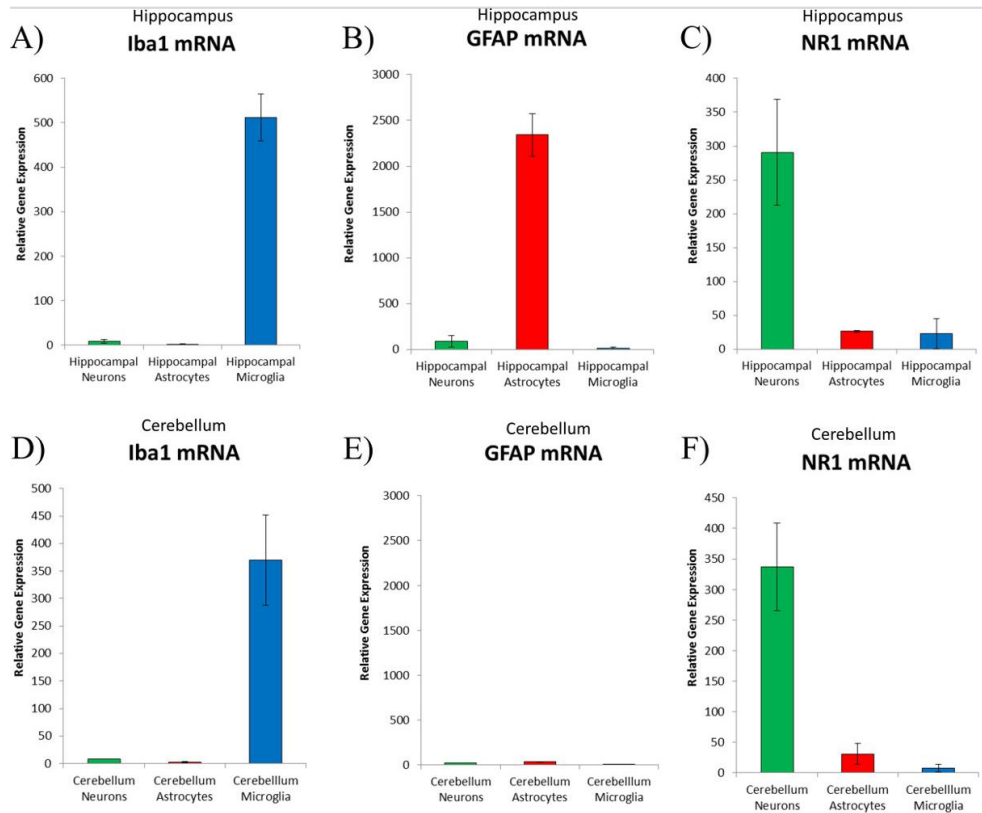




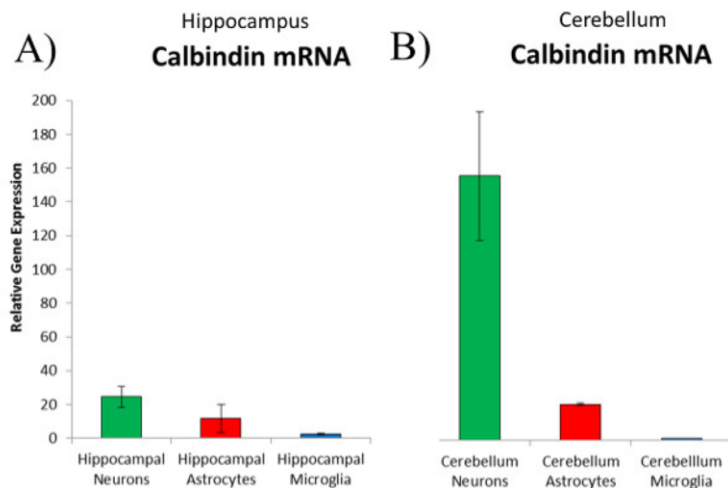
# Using Fluorescence Activated Cell Sorting to Examine Cell-Type-Specific Gene Expression in Rat Brain Tissue



**Figure 3. Neurons, astrocytes, and microglia sorted from a male hippocampus.** The hippocampus from one male rat was dissociated and stained with the antibodies for CD11b, GLUT1 and Thy1 and sorted using a FACS machine. **(A)** Cells were first sorted based on their forward and side scatter from all possible events. This gate is called P1 (population 1). **(B)** Next, single cells, also called singlets, were sorted based on their size from the doublets or larger clumps of cells. This gate is called P2. **(C)** Third, the single cells were gated as either APC-CD11b positive (CD11b+ gate, P4) or APC-CD11b negative (CD11b- gate, P3). **(D)** APC-CD11b negative cells were subsequently sorted into PE-GLUT1 positive cells (GLUT1+ gate, P6) and FITC-Thy1 positive cells (Thy1+ gate, P5). The breakdown of all events and all gates was generated from the FACS software depicted in a table which is presented on the right.



**Figure 5. Real-time PCR analysis of cell-type-specific genes from sorted cells.** Neurons (green bars), astrocytes (red bars) and microglia (blue bars) were sorted based on the protocol described above and mRNA was extracted for confirmation of cell-type-specific gene expression. **(A)** *Iba1* is a calcium binding protein expressed exclusively in **microglia** sorted from the male hippocampus. **(B)** *GFAP* is a filament protein expressed predominantly in **astrocytes** sorted from the male hippocampus **(C)** *NR1* is a ubiquitous subunit of the NMDA glutamatergic receptor that was expressed predominantly on **neurons** sorted from the male hippocampus. **(D)** *Iba1* was also expressed exclusively on microglia sorted from the male cerebellum. **(E)** Interestingly, *GFAP* was not expressed in any of the cell types sorted from the male cerebellum. **(F)** The *NR1* subunit of the NMDA receptor was also expressed predominantly on neurons sorted from the male cerebellum.

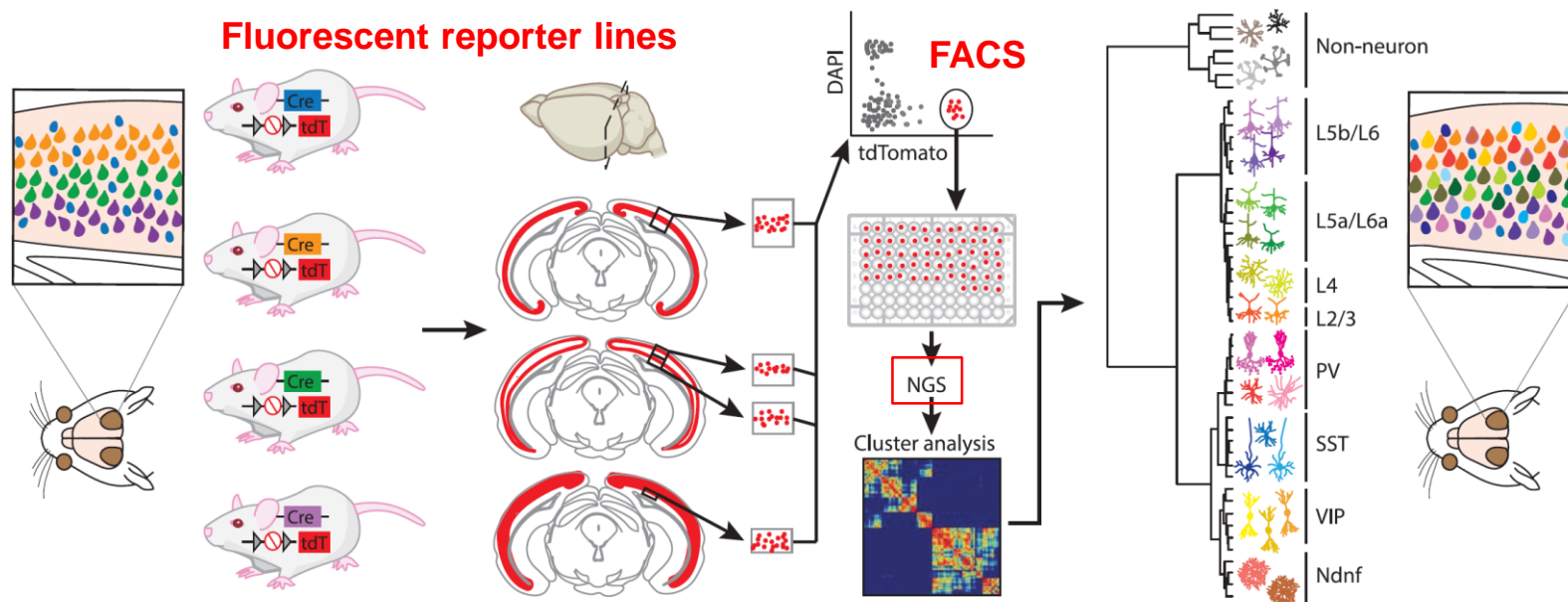


**Figure 6. Real-time PCR analysis of calbindin expressed in sorted neural cells.** Cells sorted using FACS can be used to analyze cell-type specific gene expression. **(A)** **Neurons** (green bars) expressed significantly more **Calbindin** than either astrocytes (red bars) or microglia (blue bars) sorted from the male hippocampus. **(B)** Neurons sorted from the male cerebellum expressed significantly higher levels of **Calbindin** than either astrocytes or microglia sorted from the cerebellum, but also significantly higher levels than the neurons sorted from the hippocampus.

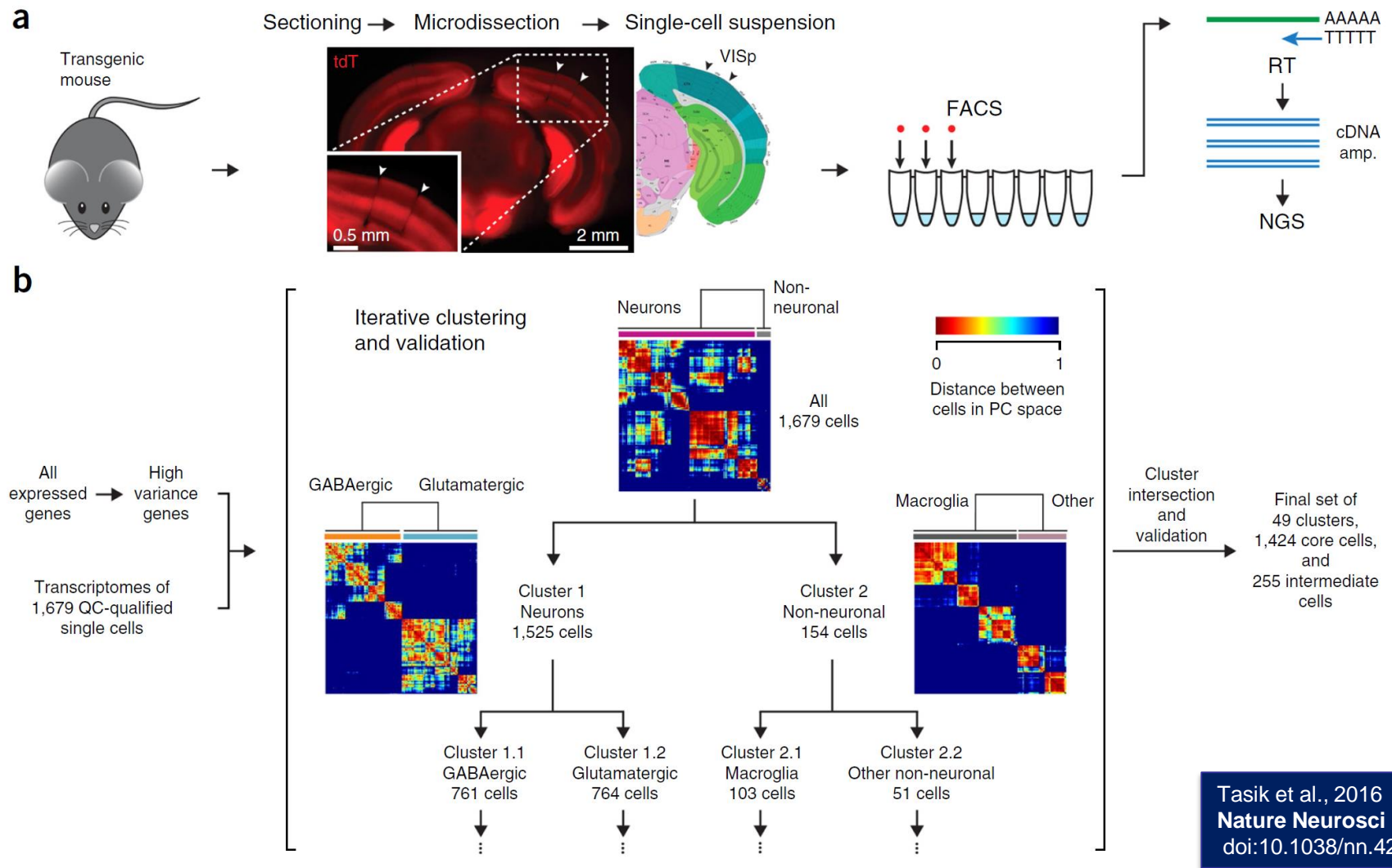
# Adult mouse cortical cell taxonomy revealed by single cell transcriptomics

Bosiljka Tasic<sup>1,2</sup>, Vilas Menon<sup>1,2</sup>, Thuc Nghi Nguyen<sup>1</sup>, Tae Kyung Kim<sup>1</sup>, Tim Jarsky<sup>1</sup>, Zizhen Yao<sup>1</sup>, Boaz Levi<sup>1</sup>, Lucas T Gray<sup>1</sup>, Staci A Sorensen<sup>1</sup>, Tim Dolbeare<sup>1</sup>, Darren Bertagnolli<sup>1</sup>, Jeff Goldy<sup>1</sup>, Nadiya Shapovalova<sup>1</sup>, Sheana Parry<sup>1</sup>, Changkyu Lee<sup>1</sup>, Kimberly Smith<sup>1</sup>, Amy Bernard<sup>1</sup>, Linda Madisen<sup>1</sup>, Susan M Sunkin<sup>1</sup>, Michael Hawrylycz<sup>1</sup>, Christof Koch<sup>1</sup> & Hongkui Zeng<sup>1</sup>

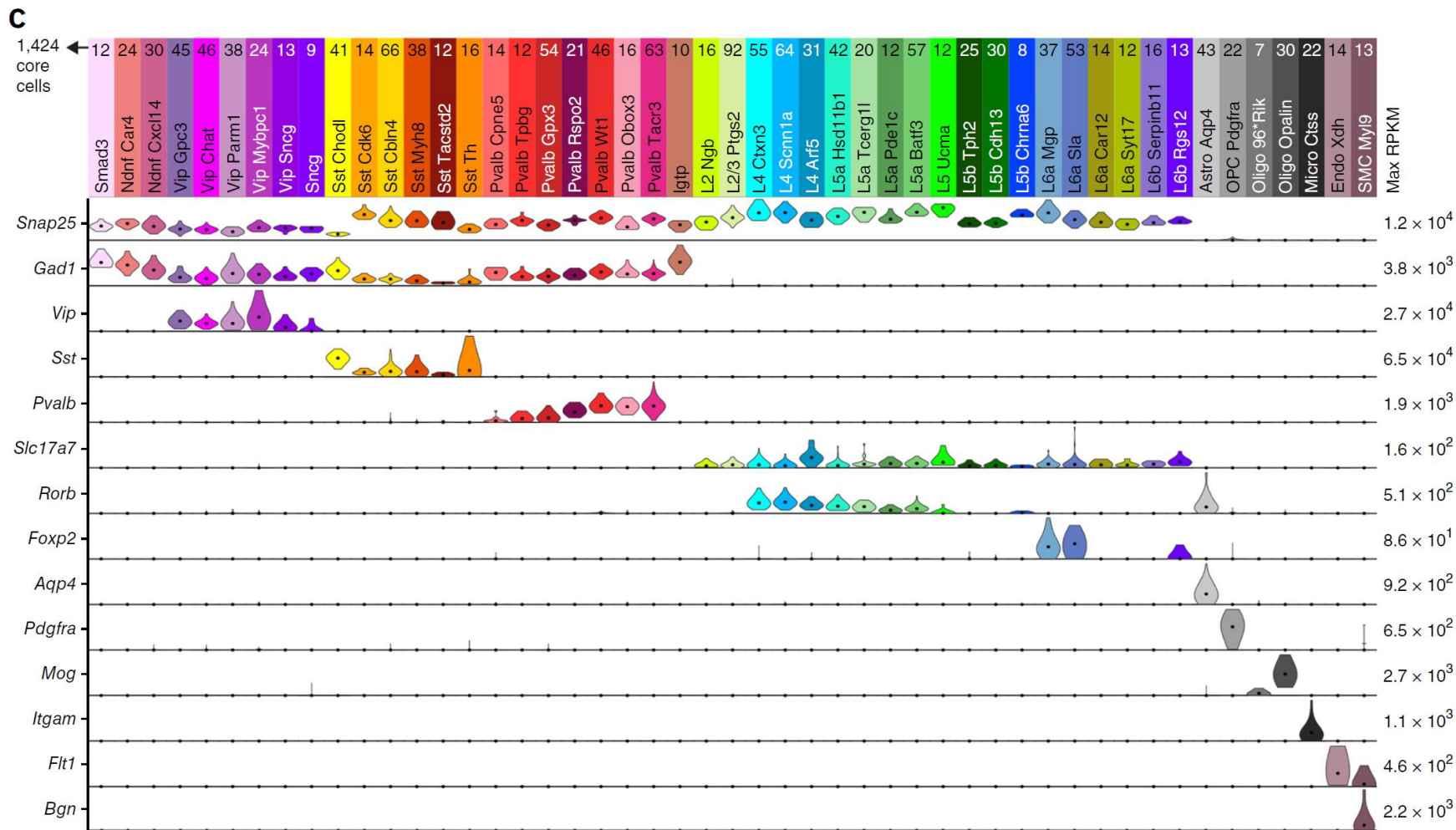
The most complete single-neuron transcriptome database of the mouse visual cortex was performed using a large collection of reporter mouse lines. Results highlight the unmatched neuronal diversity of the cerebral cortex.



**Figure 1** Single-neuron RNA-seq analysis of the adult mouse visual cortex. A large repertoire of Cre driver lines crossed to *loxP* tdTomato (tdT) reporter lines was used to label distinct neuronal populations in the mouse visual cortex. Specific layers of the primary visual cortex were microdissected from freshly sectioned adult mouse brains, and single neurons from these samples were purified by fluorescence-activated cell sorting for use in single-cell RNA-seq. Cluster analysis was conducted agnostic to the reporter line of origin. The resulting clusters were assigned to 49 transcriptionally defined cell types, 42 of them neuronal, highlighting the molecular diversity in classes of cortical excitatory and inhibitory neurons. PV, parvalbumin; SST, somatostatin; VIP, vasoactive intestinal polypeptide; Ndnf, neuron derived neurotrophic factor; NGS, next generation sequencing.



**Figure 1** Workflow overview. **(a)** Experimental workflow started with the isolation, sectioning and microdissection of the primary visual cortex from a transgenic mouse. The tissue samples were converted into a single-cell suspension, single cells were isolated by FACS, poly(A)-RNA from each cell was reverse transcribed (RT), cDNA was amplified and fragmented, and then sequenced on a next-generation sequencing (NGS) platform. **(b)** Analysis workflow started with the definition of high-variance genes and iterative clustering based on two different methods, PCA (shown here) and WGCNA, and cluster membership validation using a random forest classifier. Cells that are classified consistently into one cluster are referred to as core cells ( $N = 1,424$ ), whereas cells that are mapped to more than one cluster are labeled as intermediate cells ( $N = 255$ ). After the termination criteria are met, clusters from the two methods are intersected, and iteratively validated until all core clusters contain at least four cells (**Supplementary Fig. 3** and



Online Methods). (c) The final 49 clusters were assigned an identity based on cell location (Fig. 2) and marker gene expression (Fig. 3). Each type is represented by a color bar with the name and number of core cells representing that type. The violin plots represent distribution of mRNA expression on a linear scale, adjusted for each gene (maximum RPKM on the right), for major known marker genes: *Snap25* (pan-neuronal); *Gad1* (pan-GABAergic); *Vip*, *Sst* and *Pvalb* (GABAergic); *Slc17a7* (pan-glutamatergic); *Rorb* (mostly L4 and L5a); *Foxp2* (L6); *Aqp4* (astrocytes); *Pdgfra* (oligodendrocyte precursor cells, OPCs); *Mog* (oligodendrocytes); *Itgam* (microglia); *Flt1* (endothelial cells); and *Bgn* (smooth muscle cells, SMC).

**The Allen Brain Atlas**  
**Cellular taxonomy of the mouse visual cortex**

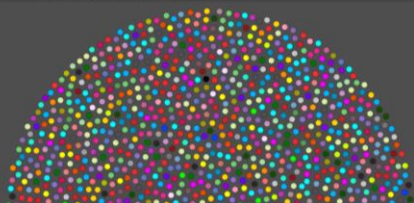
**ALLEN BRAIN ATLAS**  
DATA PORTAL

Introduction Gene Expression & Cell Taxonomy Explore the Data

A Cellular Taxonomy of the Mouse Visual Cortex

The mammalian brain is composed of various cell populations that differ based on their molecular, morphological, electrophysiological and functional characteristics. Classifying these cells into types is one of the essential approaches to defining the diversity of brain's building blocks.

We created a cellular taxonomy of the mouse primary visual cortex by analyzing gene expression patterns, at the single cell level.



**Revealing a Taxonomy**  
*Neurons and non-neuronal cells*

In the first iteration of our cluster analysis, two major cell types present themselves: neuronal and non-neuronal cells.

Contin

**Revealing a Taxonomy**  
*Non-neuronal cells*

The non-neuronal cells further segregate into endothelial cell types (in pinkish gray shades), and several glial types (e.g., microglia, astrocytes, oligodendrocyte precursor cells (OPCs) and oligodendrocytes, in gray shades).

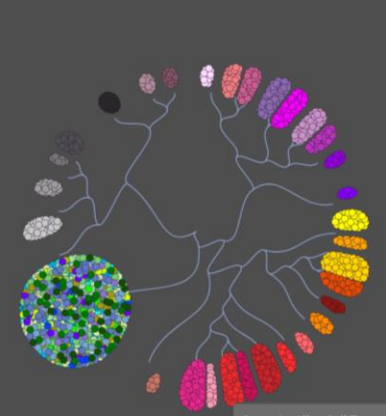
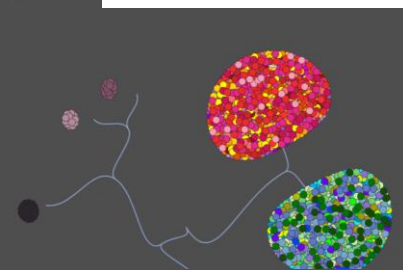
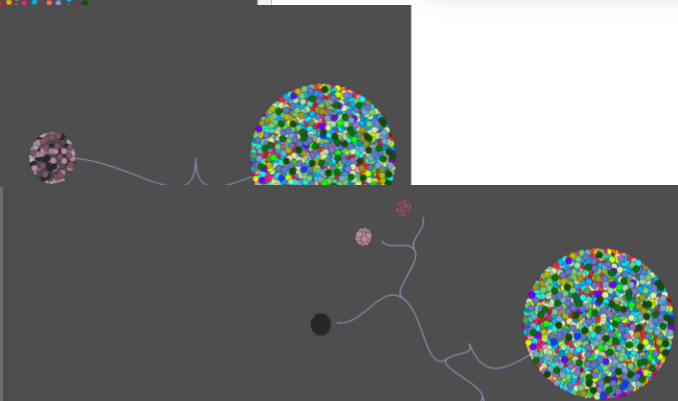
Contin

**Revealing a Taxonomy**  
*Excitatory and Inhibitory cells*

The neuronal cells segregate into two major types: the excitatory neurons (in the cooler green and blue colors) and the inhibitory neurons (in the warmer, orange and pink colors).

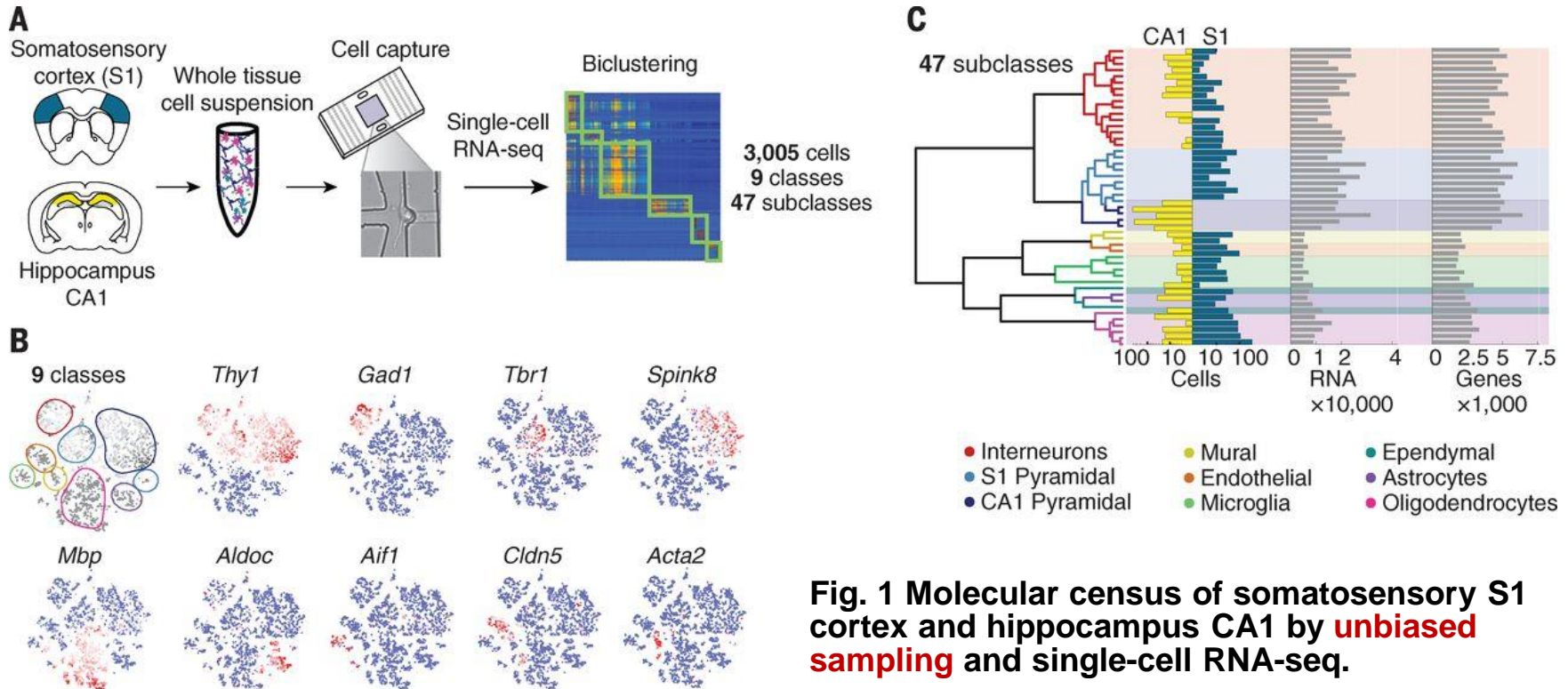
**Revealing a Taxonomy**  
*Inhibitory neurons*

Most inhibitory neurons segregate into four major clusters in agreement with specific molecular markers: parvalbumin (Pvalb), somatostatin (Sst), vasoactive intestinal polypeptide (Vip) and neuron-derived neurotrophic factor (Ndnf). Each of these major cell types further segregates into subtypes.



# Cell types in the mouse cortex and hippocampus revealed by single-cell RNA-seq\*

Zeisel et al., 2015 Science 347:1138-1142

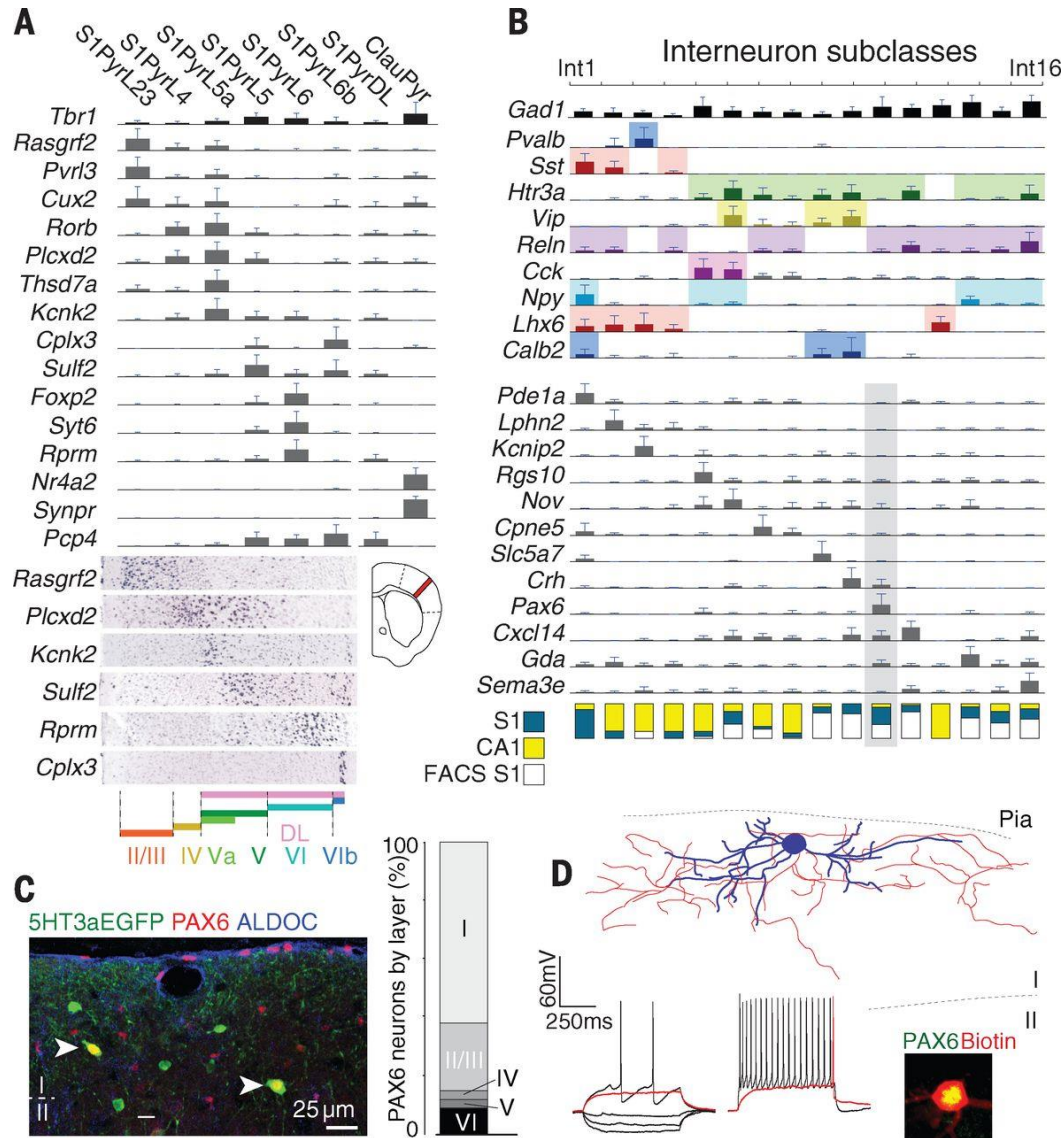


**Fig. 1 Molecular census of somatosensory S1 cortex and hippocampus CA1 by unbiased sampling and single-cell RNA-seq.**

**(A)** Workflow for obtaining and analyzing single-cell RNA-seq from juvenile mouse cortical cells, from dissection to single-cell RNA-seq and biclustering. **(B)** Visualization of nine major classes of cells using t-distributed stochastic neighbor embedding (tSNE). Each dot is a single cell, and cells are laid out to show similarities. Colored contours correspond to the nine clusters in (A) and fig. S3. Expression of known markers is shown using the same layout (blue, no expression; white, 1% quantile; red, 99% quantile). **(C)** Hierarchical clustering analysis on 47 subclasses. Bar plots show number of captured cells in CA1 and S1, number of detected polyA+ RNA molecules per cell, and total number of genes detected per cell.

\* **RNA-Seq (RNA sequencing)**, uses **next-generation sequencing (NGS)** to reveal and quantify the whole transcriptome in a biological sample. See Mutz et al., 2013 (Current Opinion in Biotechnology, 24:22–30) for review of the technique

## Fig. 2 Neuron subclasses in the somatosensory cortex



**(A)** Subclasses of pyramidal neurons in the somatosensory cortex (S1) identified by BackSPIN clustering. Bar plots show mean expression of selected known and novel markers (error bars show standard deviations). Layer-specific expression shown by in situ hybridization (Allen Brain Atlas). S1PyrL23, layer II-III; S1PyrL4, layer IV; S1PyrL5a, layer Va; S1PyrL5, layer V; S1PyrL6, layer VI; S1PyrL6b, layer VIb; S1PyrDL, deep layers; ClauPyr, claustrum.

**(B)** Identification of interneuron subclasses. Bar plots show selected known and novel markers. Fraction of S1/CA1 cells is depicted at bottom: blue, S1; yellow, CA1; white, flow-sorted Htr3a+ cells from S1.

**(C)** Immunohistochemistry demonstrating the existence and localization of novel PAX6+/5HT3aEGFP+ interneurons, Int11. Bar plots show the layer distribution of these neurons. **(D)** Intrinsic electrophysiology and morphology of PAX6+ interneurons in S1 layer I, identified by post hoc staining.